HHS Public Access

Author manuscript

Mol Neurobiol. Author manuscript; available in PMC 2020 August 01.

Published in final edited form as:

Mol Neurobiol. 2019 August ; 56(8): 5568–5585. doi:10.1007/s12035-019-1467-8.

Activation of mGluR1 mediates C1q-dependent microglial phagocytosis of glutamatergic synapses in Alzheimer's rodent models

Bihua Bie[*], **Jiang Wu**[*], **Joseph F. Foss**, and **Mohamed. Naguib**

Anesthesiology Institute, Cleveland Clinic, 9500 Euclid Ave., Cleveland, OH 44195, USA

Abstract

Microglia and complements appear to be involved in the synaptic and cognitive deficits in Alzheimer's disease (AD), though the mechanisms remain elusive. In this study, utilizing two types of rodent model of AD, we reported increased complement C1q-mediated microglial phagocytosis of hippocampal glutamatergic synapses, which led to synaptic and cognitive deficits. We also found increased activity of the metabotropic glutamate receptor 1 (mGluR1) in hippocampal CA1 in the modeled rodents. Artificial activation of mGluR1 signaling promoted dephosphorylation of fragile X mental retardation protein (FMRP) and facilitated the local translation machinery of synaptic C1q mRNA, thus mimicking the C1q-mediated microglial phagocytosis of hippocampal glutamatergic synapses and synaptic and cognitive deficiency in the modeled rodents. However, suppression of mGluR1 signaling inhibited the dephosphorylation of FMRP and repressed the local translation of synaptic C1q mRNA, which consequently alleviated microglial phagocytosis of synapses and restored the synaptic and cognitive function in the rodent models. These findings illustrate a novel molecular mechanism underlying C1q-mediated microglial phagocytosis of hippocampal glutamatergic synapses in AD.

Keywords

Alzheimer's disease; complement C1q; metabotropic glutamate receptor; fragile X mental retardation protein; microglial phagocytosis; synaptic loss

Introduction

The AD brain is characterized by extensive amyloid-induced neuroinflammation (e.g., microglia activation), neuronal and synaptic loss, and memory deficiency [1]. Dysfunction of hippocampal glutamatergic synapses markedly contributes to the cognitive impairment seen in AD patients and rodent models of AD [2,3]. Currently, the molecular and cellular mechanism underlying amyloid-induced synaptic loss is only partially understood. Microglia play a central role in the induction and maintenance of synaptic plasticity in brain

Correspondence to: Mohamed Naguib, Anesthesiology Institute, Cleveland Clinic, and Cleveland Clinic Lerner College of Medicine, Case Western Reserve University, 9500 Euclid Ave., Mail Code NB3-78,Cleveland, OH 44195, naguibm@ccf.org.

[*]These authors contributed equally to this work.

Conflict of interest:

The authors declare no conflict of interest.

neurons by altering the local environment and by modifying synaptic structure [4–7]. Phagocytosis of synapses by microglia contributes to synaptic development in mice [8] and synaptic deficit in neurological disorders including a transgenic mouse model of AD [9–12], but the underlying molecular mechanism remains elusive.

The complement system serves as the first line of defense against infection of exogenous pathogens and also clears the cellular debris to protect against autoimmunity [13]. While peripheral circulating complement proteins are mostly synthesized in the liver, many are produced locally by the resident neurons or glial cells in the brain [14]. It was previously reported that C1q, the initiating protein of the classical pathway for complement activation, was synthesized in retinal ganglion cells [15], and the complement receptor CR3 (a complex consisting of CD11b and CD18) was located exclusively in the central microglia[16,17]. Binding of C1q to apoptotic cell membranes or pathogens results in C3 opsonization and phagocytosis by macrophages expressing complement receptors [14]. C1q also contributes to synaptic pruning by tagging the weak or damaged synapses, resulting in their subsequent phagocytosis by microglia in a transgenic mouse model of neurodegenerative diseases [14,12]. The expression of C1q is substantially increased in several brain regions in the normal aging mouse and human brain [18]. Inhibition of C1q or the microglial complement receptor CR3 reduces the microglial phagocytosis of synapses and synaptic loss in the early stage (3 months old) in the transgenic AD mice [11]. The present study sought to further elucidate the critical role of C1q in the synaptic loss in rodent models of AD.

It is currently recognized that protein synthesis occurs not only in the cell soma but also in the neurites [19]. In particular, a significant amount of mRNA has been identified in the dendrites of hippocampal neurons [20], providing a mechanism for spatially restricting gene expression in a synapse-specific manner [19]. Evidence suggests that a modification of dendritic mRNA translation contributes to several neural processes such as synapse formation, learning-related synaptic plasticity, or synapse elimination [21,19,22]. Fragile X mental retardation protein (FMRP), an mRNA-binding protein abundant in the brain, modulates the transportation and local translation of synaptic mRNA[23,24], and increased FMRP expression was recently reported in the transgenic mouse AD model[25]. Metabotropic glutamate receptors (mGluRs) that are abundantly located in the excitatory synapses may, *via* the mGluR-protein phosphatase 2A (PP2A) pathway, alter the phosphorylation status of FMRP, thus modulating the translation of local mRNA [24,26]. Activation of group I mGluRs induced long-term depression [27] and was intensively involved in the amyloid-induced synaptic dysfunction in the hippocampal neurons [28,29]. Here we provide evidence that up-regulated mGluR signaling induced dephosphorylation of FMRP, and facilitated the local translation machinery of synaptic C1q mRNA, which consequently enhanced the hippocampal microglial phagocytosis of synapses and contributed to the synaptic and cognitive dysfunction in the rodent models of AD.

Materials and Methods

Animals

All animal procedures were approved by the Animal Care and Use Committee of Cleveland Clinic. Adult male Sprague–Dawley (250–300 g, 2–3 mo of age, Charles River) rats were

used, and all experiments were performed during the light cycle. Tg-APPsw/PSEN1DE9 (APP/PS1, MMRRC Stock No: 41848-JAX), and C57BL/6 mice were purchased from Jackson Laboratory, regularly maintained and studied at six months old. Tg-APPsw/PSEN1DE9 mice were obtained as hemizygote by crossing the transgenics with animals on a C57BL/6 background. During experiment, non-transgenic littermates were used as the control for the transgenic mice with the same age (6 months old) and gender ratio (male/female ratio about 1). Metabotropic glutamate receptor 1 mutant mice (*Grm1*$^{-/-}$, C57BL/6J-*Grm1*$^{rcw-3J}$/GrsrJ, Jackson Laboratory stock No. 005521) crossed with APP/PS1 mice to generate the new strain (APP/PS1/*Grm1*$^{-/-}$), which was validated by genotyping following the protocols provided by Jackson Laboratory. Experiments were conducted in mice at the age of 6 mo. The animals were randomly assigned to different groups with specific treatment, and another party blinded the experimenter to the individual groups. No statistical methods were used to predetermine sample sizes, but our sample sizes are similar to those reported in previous publications [30,3].

Microinjection in the hippocampal CA1 area

The rats were anesthetized with sodium pentobarbital (45 mg/kg i.p.) and restrained in a stereotaxic apparatus[31]. A$\beta_{1–40}$ fibrils were formed as described previously [32]. A$\beta_{1–40}$ fibrils (10 μg/3μl), A$\beta_{40–1}$ fibrils (10 μg/3μl) or 3μl of artificial cerebrospinal fluid were injected stereotaxically and bilaterally into each hippocampus (anteroposterior: −3.5 mm, mediolateral: ± 2.0 mm, dorsoventral: −3.0 mm) [33] using a 10 μl Hamilton syringe with a 27 G stainless steel needle at a rate of 0.5 μl /min. Our previous immunostaining studies confirmed the deposition of A$\beta_{1–40}$ species in hippocampal CA1 14 days after the microinjection in the modeled rats [3,34–36]. It has been shown that Aβ1-$_{40}$ species co-exist with A$\beta_{1–42}$ species in the brain of APP/PS1 mice [37–39]. The experimental model using A$\beta_{1–40}$ species has been used for studying AD [40,41,32,35,36,3].

For *in vivo* treatment by microinjection, a 26-gauge double-guide cannula was inserted into the brain, aimed at the hippocampal CA1 area (same coordinate as above) [31]. The guide cannula was then cemented in place to the skull and securely capped. The rat was allowed to recover for at least 5 d before subsequent treatment. C1q siRNA and scrambled RNA (scRNA) were commercially designed and synthesized by Invitrogen. All types of siRNA (5 nmol in 3 μl/side), specific mGluR agonist dihydroxyphenylglycine (DHPG; 0.25 μg/side), JNJ16259685 (0.3 ng/side), or artificial CSF were delivered daily into the hippocampal CA1 area through a 33 gauge double injector at a rate of 0.5 μl/min for 7 days. Behavioral, cellular and molecular analysis were performed one day after the last injection of specific agents or vehicle. The injection sites for the hippocampal CA1 were histologically verified afterward by injecting the same dose of ink [42,35].

Morris water maze test

The Morris water maze test (n = 10 in each group) was employed to determine the memory function of the rats and mice [32,35,43,44]. The water maze model was performed in a circular tank (diameter 1.8 m for rats and 1.32 m in diameter for mice) filled with opaque water. A platform (15 cm in diameter) was submerged below the water's surface in the center of the target quadrant. The swimming path of the animal was recorded by a video

camera and analyzed by EthoVision XT software (Noldus Information Technology). Each rat underwent 4 trials per day for 5 days. The mice were tested in the visible platform (for 3 days) and the hidden platform (for 4 days) task of the Morris water maze. They underwent four trials a day for seven days with a 10 min inter-trial interval. For each training session, the animals were placed into the maze consecutively from four random points of the tank, and were allowed to search for the platform. If the animal did not find the platform within (120 s for rats and 60 s for mice), they were gently guided to it. Animals were allowed to remain on the platform for 20 s. The latency for each trial was recorded for analysis. During the probe trial, the platform was removed from the tank and the rats were allowed to swim in the maze for 60 s.

Hippocampal synaptosomal preparation

Hippocampal synaptosome preparations were obtained as previously described [22]. Hippocampal CA1 tissues from the rats in the appropriate groups were gently homogenized in ice-cold 0.32 M sucrose buffer with proteinase and phosphatase inhibitors at pH 7.4 and then centrifuged for 10 min at 1,000g (4°C). The supernatant was collected and centrifuged for 20 min at 10,000g (4°C). The synaptosomal pellet was then collected and proceeded to the subsequent mRNA and protein analysis.

Protein extraction and immunoblotting

The protocol for protein extraction and immunoblotting was generally based on previous reports [45,31]. The hippocampal CA1 tissues or synaptosomal preparations were collected and lysed in ice-cold lysis buffer containing 50 mM Tris–Cl, 150 mM NaCl, 0.02 mM NaN_2, 100 μg/ml phenylmethyl sulfonyl fluoride, 1 μg/ml aprotinin, 1% Triton X-100 and proteinase and phosphatase inhibitor cocktail. The proteins were extracted and subjected to 7.5% - 15% SDS– PAGE followed by immunoblotting. The blots were incubated overnight at 4 °C with the primary antibodies as follows: monoclonal anti-C1q antibody (1:1000; Abcam, ab71940), anti-FMRP antibody (1:1000; Cell Signaling, 7104), monoclonal anti-p-FMRP antibody (1:1000; Thermo Scientific, PA5–35389), and monoclonal anti-β-actin antibody (1:2000; Santa Cruz Biotechnology, sc-81178). The membranes were washed extensively and then incubated with horseradish peroxidase (HRP) -conjugated anti-mouse and anti-rabbit IgG antibody (1:10,000; Jackson ImmunoResearch Laboratories Inc., West Grove, PA). The immunoreactivity was detected using enhanced chemiluminescence (ECL Advance Kit; Amersham Biosciences). The intensity of the bands was captured digitally and analyzed quantitatively with ImageJ software. The immunoreactivity of all proteins was normalized to that of β-actin.

RNA immunoprecipitation (RNA-IP) and quantitative RT-PCR for mRNA analysis

RNA-IP was performed in the hippocampal tissue as previously described [46]. Briefly, the hippocampal CA1 tissue was collected and homogenized in the lysis buffer. Protein/mRNA complex was precipitated by the monoclonal anti-p-FMRP (1:100, Thermo Scientific, PA5–35389) antibody or anti-eIF-4E antibody (1:100, Cell Signaling, 9741) and was recovered with protein A/G beads. The pulled-down and input mRNA was extracted using a single-step RNA isolation protocol and quantified as previously described [47]. GAPDH was used internal control [48,49]. Reverse transcription and real-time RT-PCR were performed in

triplicate with C1q primers (5′- ACAAGGTCCTCACCAACCAG −3′, 5′- CGTTGCAATTGAAGCACAGT −3′), and GAPDH primers (5′- AGACAGCCGCATCTTCTTGT −3′, 5′- CTTGCCGTGGGTAGAGTCAT −3′). IP/input ratio was then calculated. For the analysis of C1q mRNA in the synaptosomal preparation, fold change was calculated using the ΔΔCT method. The entire protocol was repeated in triplicate, and the mean and SEM were calculated.

Immunostaining and 3-D confocal imaging

Immunostaining on the serial sections containing hippocampal CA1 area in all groups (30 μm, 15–20/rat, n = 5 rats per group) was performed as previously described [31,35]. Mouse monoclonal antibody against the microglial marker Iba1 (1:500, Abcam, ab5076), glutamatergic presynpatic marker synaptophysin (1:200, Cell signaling, 5467), C1q (1:200, Abcam, ab71940), CD68 (1:500, Abcam, ab955), goat anti-PSD-95 (1:500, Abcam, ab12093), rabbit anti-PSD95 (1:500, Cell Signaling, 3450), rabbit anti-FMRP (1:500, Cell Signaling, 7104), and rabbit anti-pFMRP (1:400, Thermo Scientific, PA5–35389) were used. The sections were then incubated with FITC-, Cy3-conjugated secondary antibody (1:500, Jackson ImmunoResearch), or Alex Fluor 633 (1:500, Invitrogen) for 1 h. Mouse IgG isotype (Abcam, ab188776) was applied as control of C1q immunostaining in the same groups of tissues as above. Negative controls were run in parallel, and involved omission of one or both primary antibodies and/or inclusion of an irrelevant isotype control antibody. All such controls were devoid of staining. All sections were examined by the confocal microscopy, and fluorescent images were acquired using a Leica TCS-SP8-AOBS inverted confocal microscope (Leica Microsystems, GmbH, Wetzlar, Germany). Image rendering and analyses were performed using Image-Pro Plus (Media Cybernetics, Inc., Rockville, MD) and Velocity (PerkinElmer, Waltham, MA). The presentation and analysis of internalization of PSD95 or synaptophysin in microglial (Iba1) lysosomes (CD68) were adopted from the method described by Schafer, et al.[6] with minor modification. Briefly, the internalization of PSD95 or synaptophysin in microglial lysosomes was defined by rotating the 3D micrographs to confirm the colocalization of synaptic markers with CD68 immunoreactivity within microglia in hippocampal CA1. The representative 3D images were presented with resolution 1024 × 1024 dpi, z-step size 0.3 μm. Usually, a 200 × 200 ×20 μm neuropil (containing about 9–12 microglia) in each section and 4 sections in each animal were randomly sampled and analyzed in different groups. The volume of PSD95 or synaptophysin within lysosome (CD68-positive) and the total volume of these synaptic markers in a neuropil (200 μm × 200 μm × 20 μm) were measured by Velocity (PerkinElmer, Waltham, MA), and the ratio was calculated as the measurement of microglial phagocytosis of synapses in hippocampal sections in all groups using the following formula: PSD95 engulfment (%) = volume of CD68 -positive PSD95 puncta (μm^3)/volume of total PSD95 (μm^3) × 100.

Hippocampal slice preparation and whole-cell recordings

Brain slices containing hippocampal CA1 areas were prepared as previously described [31,50,42]. The brain was quickly removed and cut on a Vibratome in cold physiological saline to obtain coronal slices (300 μm thick) containing the hippocampus. Whole-cell voltage-clamp recordings from the CA1 area were taken using an Axopatch 200B amplifier

(Molecular Devices) with 2–4 MΩ glass electrodes containing the internal solution (mM): K-gluconate or cesium methanesulfonate, 125; NaCl, 5; $MgCl_2$ 1; EGTA, 0.5; Mg-ATP, 2; Na_3GTP, 0.1; HEPES, 10; pH 7.3; 290–300 mOsmol. A seal resistance of ≥ 2 GΩ and an access resistance of 15–20 MΩ were considered acceptable. The series resistance was optimally compensated by ≥ 70% and constantly monitored throughout the experiments. Schaffer collateral–commissural fibers were stimulated by ultrathin concentric bipolar electrodes (FHC Inc.), and the excitatory postsynaptic currents (EPSCs) were recorded in the CA1 area in the presence of bicuculline (30 μM). The evoked EPSCs were filtered at 2 kHz, digitized at 10 kHz, and acquired and analyzed using Axograph X software. The amplitude of the EPSCs was monitored for a baseline period of at least 15 min. Miniature EPSC (mEPSC) was recorded in the presence of tetrodotoxin (TTX, 1 μM) and bicuculline (10 μM) at a holding potential of −70 mV. All electrophysiological experiments were performed at room temperature.

Compounds and statistical analyses

Aβ peptide consisting of residues 1–40 of the human wild-type sequence ($Aβ_{1–40}$) and $Aβ_{40–1}$ was purchased from Bachem (Torrance, CA). AP-5 (D-2-amino-5-phosphonopentanoate), CNQX (6-cyano-2,3-dihydroxy-7-nitroquinoxaline), bicuculline, and other chemicals were purchased from Sigma Aldrich (St. Louis, MO) or Tocris (Ellisville, MO).

Normality was tested using the Shapiro-Wilk test. For electrophysiological and behavioral analysis, the data were compared with two-way ANOVA. The data from the histological study, western blot, real-time PCR and other studies were analyzed using Student's *t*-test, one-way ANOVA test. For non-normally distributed data we used Mann-Whitney U test, or Kruskal-Wallis test. *Post hoc* analyses were performed using Student-Newman-Keuls test or Dunn multiple comparisons test as appropriate. All statistical analyses were performed with BMDP statistical software (Statistical Solutions, Saugus, MA). All data were expressed as means ± SEM. For all tests, a two-tailed $P < 0.05$ was considered statistically significant.

Results

Microglial Phagocytosis of Glutamatergic Synapses Induced by Amyloid Fibrils.

Consistent with our previous studies [3,35,36], bilateral microinjection of $Aβ_{1–40}$ fibrils (but not of reverse sequence $Aβ_{40–1}$ fibrils or artificial CSF) into the hippocampal CA1 led to memory deficiency, as shown by extended escape latencies and less time spent in the target quadrant (during the probe trial) in the Morris water maze test (Fig. 1a,1b). We also observed a substantial rightward shift in the input (stimulation intensities) - output (current amplitudes) curve of glutamatergic excitatory post-synaptic currents (EPSCs) in the hippocampal CA1 neurons in the modeled rats (Fig. 1c). Further analysis of the miniature postsynaptic currents revealed a significant decrease in the amplitude and increase of the inter-event interval of excitatory glutamatergic transmission in the hippocampal CA1 neurons in these modeled rats (Fig. 1d). Notably, our previous report also demonstrated a reduction of hippocampal dendritic spine numbers using Golgi impregnation staining and a substantially decreased immunosignal of presynaptic marker vGluT1 in the hippocampal

CA1 in the rats injected with $A\beta_{1–40}$ fibrils [3]. These results demonstrated a substantial suppression of hippocampal glutamatergic transmission in the rats injected with amyloid fibrils.

Microinjection of $A\beta_{1–40}$ fibrils also increased the intensity of Iba1 and CD68 (a microglial lysosomal marker), indicating an extensive microglial activation and neuroinflammation in the hippocampal CA1 (Fig. 1e,f). To determine the involvement of activated microglia in the suppressed hippocampal neurotransmission, the microglial phagocytosis of glutamatergic synapses was evaluated by immunostaining with antibodies against postsynaptic marker PSD95, microglial marker Iba1 and the lysosomal marker CD68 in the hippocampal CA1 in the modeled rodents. We found that the majority of PSD95 immunosignals within microglia were co-localized within lysosomal compartments in rats injected with $A\beta_{1–40}$ fibrils, but not those injected with $A\beta_{40–1}$ fibrils (Fig. 2a), and APP/PS1 mice (Fig. 2b). Internalization of PSD95 within microglial lysosomes was further confirmed by assessing confocal z stacks through individual microglia in AD models of rat (Movie 1) and mice (Movie 2). Consistently, internalization of another synaptic marker synaptophysin with lysosomes in microglia was also observed in the hippocampal CA1 in the modeled rats when compared with those injected with saline or with $A\beta_{40–1}$ fibrils (Fig. 3a). This was also observed in APP/PS1 mice when compared to wild type mice (Fig. 3b). Taken together, these results support a role of microglial phagocytosis in glutamatergic synapse loss in the rodent models of AD.

Complement C1q mediates the microglial phagocytosis of glutamatergic synapses

Previous findings provided clues that complement C1q is a key mediator of synaptic loss in neurodegenerative disorders including multiple sclerosis [51] and early stages of AD in rodent models [11]. Here we explored the role of C1q-mediated microglial phagocytosis of glutamatergic synapses in AD. In accordance with a previous report[11], our results showed an increased expression of C1q in the hippocampal CA1 synaptosomal preparation in the rats injected with $A\beta_{1–40}$ fibrils (Fig. 4a), which was predominantly co-localized with the immunosignal of postsynaptic marker PSD95 (Fig. 4b, Movie 3). The increase of C1q expression was not observed in rats injected with $A\beta_{40–1}$ fibrils (Fig. S1, Fig. 4b). Note that the existence of significant C1q immunosignal outside that of PSD95 indicates the potential C1q production from other cells such as microglia or astrocytes. The expression of C1q was also increased in the hippocampal CA1 synaptosomal preparation of the APP/PS1 transgenic mice (Fig. 4c).

We then assessed whether suppressing C1q upregulation, by local administration of a specific C1q small interfering RNA (siRNA), would confirm the involvement of C1q in microglial phagocytosis of glutamatergic synapses in the presence of amyloid fibrils. Local administration of a specific C1q siRNA (5 nmol per side for 7 days), but not scrambled RNA (scRNA), effectively attenuated hippocampal C1q expression in the amyloid-injected (Fig. 4a,b) and control group as well (Fig. S1). It also decreased the localization of PSD95 within the microglial lysosomes (Fig. 5a) in the hippocampal CA1 in the modeled rats. Moreover, treatment with C1q siRNA, but not scRNA, restored the amplitude and inter-event interval of mEPSCs in the hippocampal CA1 neurons of the amyloid-injected rats (Fig. 5b). In the

Morris water maze test, the amyloid-injected rats exhibited significantly shortened escape latencies (Fig. 5c) and spent more time in the target quadrant (Fig. 5d) after treatment with C1q siRNA. Considering the potential function of C1q to initiate the complement response leading to C3 opsonization and phagocytosis, these results further confirmed the critical role of C1q signaling in the mechanism underlying amyloid fibril-induced elimination of glutamatergic synapses by microglia.

Metabotropic glutamate receptor 1 (mGluR1)-mediated synaptic C1q mRNA translation induced by amyloid fibrils

Given that neuronal protein synthesis intensively occurs at the synaptic terminals as well as cell bodies[21,22] and that phosphorylation of FMRP, *via* associated polyribosomes, may substantially impair mRNA transportation into dendrites and its translation in the synapses [26,24], we next evaluated the expression of *C1q* mRNA in the hippocampal CA1 synaptosomal preparation of amyloid-injected rats. First, we detected a substantially increased expression of hippocampal mGluR1 in rats injected with $A\beta_{1–40}$ fibrils (Fig. 6a), but not those injected with $A\beta_{40–1}$ fibrils (Fig. S2), and in APP/PS1 transgenic mice (Fig. 6b). Then, upregulation of *C1q* mRNA was observed in the synaptosomal preparation in hippocampal CA1 in the modeled rats (Fig. 6c). In addition, our RNA immunoprecipitation (RNA-IP) study revealed an increased binding of eIF-4E with *C1q* mRNA in the hippocampal synaptosomal preparation in the modeled rats (Fig. 6d). These findings suggest an enhanced translational activity of synaptic C1q mRNA in the modeled rats.

Next, we observed a corresponding reduction of phosphorylated FMRP (p-FMRP), but not the total FMRP, as measured by western blot analysis (Fig. 6e). Moreover, an RNA-IP study also revealed a significantly decreased binding of p-FMRP in the ribosome containing *C1q* mRNA in the hippocampal CA1 tissue of the amyloid injected rats (Fig. 6f). Considering the critical role of p-FMRP in modulating the local mRNA transport and translation, these results point toward FMRP involvement in the altered local expression of C1q in the hippocampal synaptosomes in the amyloid-treated rats.

Next, we also found that local administration of mGluR1 inhibitor, JNJ16259685 (0.3 ng for 7 days), significantly attenuated the dephosphorylation of FMRP (Fig. 6e) in the synaptosomal preparation of hippocampal CA1 in the modeled rats. It also increased the binding between p-FMRP and *C1q* mRNA (Fig. 6f) and decreased the upregulation of *C1q* mRNA (Fig. 6c) and C1q immunosignal and its co-localization with PSD95 (Fig. 6g). Further, results of our immunostaining study also showed that inhibition of mGluR1 signaling by JNJ16259685 significantly decreased the localization of PSD95 within microglia lysosomes (CD68) (Fig. 7a) in the hippocampal CA1 in the rats injected with $A\beta_{1–40}$ fibrils. Consistently, JNJ16259685 also significantly recovered the amplitude and inter-event interval of mEPSCs in hippocampal CA1 neurons (Fig. 7b) in the hippocampal CA1, and improved the performance in the Morris water maze test in the rodent model of AD (Fig. 7c,d).

Moreover, to confirm the role of mGluR1 in microglial phagocytosis of synapses in rodent models of AD, we crossed APP/PS1 mice with mGluR1 knockout mice ($Grm1^{-/-}$), and analyzed the C1q production and microglial phagocytosis of synapses in this new strain

(APP/PS1/*Grm1*$^{-/-}$). Consistently, substantial amelioration of p-FMRP dephosphorylation (Fig. 8a), C1q upregulation (Fig. 8b), and co-localization of PSD95 within the lysosomes (CD68) in microglia (Iba1) (Fig. 8c), as well as restoration of glutamatergic synaptic transmission (Fig. 9a) and improved performance in Morris water maze test (Fig. 9b,c) was observed in the APP/PS1/*Grm1*$^{-/-}$ mice, when compared to APP/PS1 mice. Together, our findings show that inhibition of mGluR1 signaling decreased the local translation of synaptic *C1q* mRNA, mitigated microglial phagocytosis of the glutamatergic synapses and restored synaptic strength and cognition in rodent models of AD.

The next step was to determine whether artificial activation of mGluR1 signaling mimicked the C1q-mediated microglial elimination of glutamatergic synapses similar to that noted with amyloid fibrils. We microinjected the mGluR1 agonist dihydroxy phenylglycine (DHPG, 0.25 μg per side for 7 days) into the hippocampal CA1 tissue of naïve rats and observed significantly decreased FMRP phosphorylation in the hippocampal synaptosome in the naïve rats (Fig. 10a). DHPG also decreased the binding between p-FMRP and *C1q* mRNA (Fig. 10b), and consequently upregulated the *C1q* mRNA (Fig. 10c) in the hippocampal CA1 synaptosomal preparation in the naïve rats. The increased expression of C1q was predominantly co-localized with the postsynaptic marker PSD95 (Fig. 10d) indicating its distribution in the glutamatergic synapses. We also found that activation of mGluR1 signaling by DHPG increased the localization of PSD95 within microglial lysosomes (CD68) (Fig, 11a), and decreased the amplitude and increased the inter-event interval of mEPSCs in the hippocampal CA1 neurons (Fig. 11b). Furthermore, these rats exhibited significantly extended escape latencies and spent less time in the target quadrant in the Morris water maze test (Fig. 11c,d). Taken together, these findings strongly support the critical role of upregulated mGluR1 signaling in the C1q-mediated microglial preferential elimination of glutamatergic synapses induced by amyloid fibrils.

Discussion

Reactive microglia appear to play a cardinal role in several neuroinflammatory disorders including Alzheimer's disease [52,11,3]. We have previously shown that amyloid fibril-induced microglial activation and neuroinflammation enhanced the interaction between the transcriptional repressors and suppressed the expression of synaptic scaffolding protein neuroligin 1, thus leading to the reduction of hippocampal glutamatergic synapses [3]. Reactive microglia may prune the synapses and sculpt the neural circuit, thus affecting the synaptic development and maturation in the developing nervous system [6,8]. Deficient microglianeuronal interaction has been shown to impair the synaptic pruning and functional brain connectivity, which was associated with deficits in social interaction and increased repetitive-behavior phenotypes in rodents [53]. Transient cerebral ischemia increased the duration of microglia-synapse contacts, which was frequently followed by the loss of the presynaptic buttons and contributed to the subsequent increased turnover of synaptic connections in the cortex neurons [54]. Nanomolar concentrations of Aβ induced remarkable microglial phagocytosis of neurons and synapses in culture [55]. Knockout of microglial CX3CR1, which is essential for microglial recruitment, significantly prevented neuron loss in the transgenic mice AD model [56]. Reactive microglia may inappropriately phagocytose the synapses and lead to synaptic loss in the early stage of AD mouse model

[11]. It was recently reported that sustained, but delayed, activation of microglia/macrophage and neuroinflammatory response coincided with significant tissue loss induced by traumatic brain injury in a transgenic mice model with cerebral amyloidosis [57,58]. In the present study, we also noted that reactive microglia phagocytosed the hippocampal glutamatergic synapses, which was associated with hippocampal synaptic dysfunction and memory deficiency in the established rodent models of AD. We observed synaptic and behavioral deficits in APP/PS1 mice at 6 months old in the present study, which was consistent with the other reports that synaptic loss and impaired performance in cognitive behavioral tests gradually developed as early as 3 to 6 months of age in APP/PS1 mice [59–63,11,64].

C1q-mediated synaptic elimination is involved in the pathogenesis of several neurological disorders. For instance, we noted that transforming growth factor β from astrocytes upregulated the C1q expression in retinogeniculate synapses, thus opsonizing the synapse for microglial elimination during synaptic remodeling in the mouse retinogeniculate system[15]. Increased C1q expression was temporally correlated with a decrease in synapse density in the inner plexiform layer of the retina in the rodent model of glaucoma [65]. In addition, a significantly increased spinal expression of complement C1q was detected, which potentially contributed to the synaptic elimination, in the mice model of chronic spinal cord compression[66]. Upregulation of C1q is likely associated with the disruption of neuromuscular junction architecture and impairment of sensory-motor circuitry in the neurodegenerative disease spinal muscular atrophy [67]. It was also found that C1q knockout mice exhibited defects in neocortical synapse elimination resulting in enhanced excitatory synaptic connectivity and epileptic activity [68].

Results of a recent study revealed that expression of C1q was dramatically increased in close proximity to synapses in several brain regions, including the hippocampus and cortex, in the normal aging mouse and human brain [18]. It was found that aged C1q-deficient mice exhibited significantly less cognitive and memory decline in certain hippocampus-dependent behavior tests with enhanced synaptic plasticity and reorganization of the circuitry in the aging hippocampal neurons [18]. The C1q content was found to be largely region-specifically elevated, particularly in the hippocampus and frontal cortex, and was associated with the early microglia-mediated synaptic loss in two transgenic mice models of AD (J20 and APP/PS1 mice)[11]. The present studies demonstrated a significant increase of hippocampal C1q immunosignal in the hippocampal glutamatergic synapses in the rodent models of AD, and suppression of C1q upregulation substantially attenuated the microglial phagocytosis of glutamatergic synapses, restored the hippocampal glutamatergic transmission and cognitive function in the rats injected with amyloid fibrils. Previous *in situ* hybridization studies confirmed neuronal expression of C1q in the hippocampus and cortex neurons [69–72] and brain microglial cells [73]. We also found that some C1q immunoreactivity was not co-localized with that of synaptic marker, which indicated that C1q expression from other resources (e.g., microglia) might also contribute to the pathological process seen in the present study. It is well recognized that C1q-involved complement activation serves as the first step of the classical complement cascade in a sequential manner, including C3 convertase activation and amplification, C5 convertase activation, and the assembly of the terminal complement complex [74]. Consistent with the finding of C1q-mediated microglia phagocytosis of glutamatergic synapses, previous studies

also found that genetic deletion of complement C3 or its receptor CR3 substantially ameliorated the hippocampal synaptic loss in APP/PS1 mice or mice infused with oligomeric Aβ [11]. Taken together, these findings confirmed the critical role of activation of C1q, potentially partnering with C3 and CR3 and other components in complement cascade, in microglia phagocytosis and central glutamatergic synapse loss and its functional significance in the rodent models of AD.

Previous studies demonstrated that FMRP regulated the transportation and local translation of dendritic mRNA in the central neurons [24,26]. Phosphorylation of FMRP (Ser^{499}) is associated with stalled polyribosomes, and dephosphorylated FMRP is released from the polyribosome, which facilitates the transportation and translation of local mRNA [75]. Ablation of FMRP leads to excessive and dysregulated mRNA translation at the synapse, resulting in altered synaptic function and loss of protein synthesis-dependent synaptic plasticity [76,24]. Increased expression of FMRP was reported in the transgenic mice model of AD [25]. FMRP was suggested to be involved in modulating the expression of amyloid precursor protein and in the accumulation of amyloid aggregations in the brain [77,78]. In the present study, a significant decrease of p-FMRP, as well as a reduced binding between the p-FMRP and *C1q* mRNA, was observed in the hippocampal synaptosome in the modeled rodents. Suppression of p-FMRP dephosphorylation by inhibition of mGluR1 signaling decreased the synaptic C1q expression and microglial phagocytosis of synapses, and led to recovery of glutamatergic transmission and cognition in the amyloid fibril-injected rats.

Metabotropic glutamate receptors are abundantly present in excitatory synapses throughout the brain where they regulate activity-dependent dendritic protein synthesis and glutamatergic neurotransmission. Signaling by mGluR1/5 contributes to the formation of synaptic circuits during development and is implicated in the induction of synaptic plasticity and associative learning [79]. It was reported that brain expression of mGluRs was increased in the mouse model of AD [28], and activation of mGluRs mediated the amyloid-induced suppression of synaptic plasticity in the hippocampal neurons [29]. In addition, sustained suppression of group II mGluRs markedly reduced the brain Aβ monomers and oligomers, promoted hippocampal neurogenesis and improved the anxiety and memory deficit in the transgenic mice model of AD [80]. Notably, stimulation of mGluRs also affected the phosphorylation status of FMRP, thus modulating the translation of dendritic mRNA in several physiological and pathological scenarios [26,24]. In the present study, substantially increased expression of mGluR1 signaling was demonstrated in the hippocampal CA1 in the amyloid fibril-injected rats and APP/PS1 transgenic mice. Artificial activation of mGluR1 signaling largely mimicked the amyloid-induced C1q upregulation, microglial phagocytosis of synapses, and glutamatergic and cognitive dysfunction. In contrast, knockout of mGluR1 or inhibition of mGluR1 signaling substantially recovered these molecular, cellular and behavioral impairments in the rodent AD model. Taken together, our data demonstrated a critical role of mGluR1 signaling in C1q-dependent microglial phagocytosis of synapses, but we cannot exclude the potential involvement of other receptor subtypes (e.g., mGluR5) since mGluR1 modulators (e.g., DHPG and JNJ16259685) also act on mGluR5 receptors [81,82].

Conclusion

The present study illustrates a novel mechanism–activation of mGluR1 signaling induced the C1q-mediated microglial phagocytosis of glutamatergic synapses, which contributes to the synaptic and cognitive deficiency in the rats injected with amyloid fibrils (Fig. 12).

Supplementary Material

Refer to Web version on PubMed Central for supplementary material.

Acknowledgements

Dr. Naguib is supported by the National Institute of Aging of the National Institutes of Health under Award Number R56AG051594.

This work utilized the Leica SP8 confocal microscope that was purchased with funding from National Institutes of Health SIG grant1S10OD019972-01. The authors thank John Peterson, Ph.D., Imaging Core, Cleveland Clinic for his expertise and help provided for imaging analysis.

References

1. Shankar GM, Li S, Mehta TH, Garcia-Munoz A, Shepardson NE, Smith I, Brett FM, Farrell MA, Rowan MJ, Lemere CA, Regan CM, Walsh DM, Sabatini BL, Selkoe DJ (2008) Amyloid-beta protein dimers isolated directly from Alzheimer's brains impair synaptic plasticity and memory. Nature medicine 14 (8):837–842. doi:10.1038/nm1782
2. Sun B, Halabisky B, Zhou Y, Palop JJ, Yu G, Mucke L, Gan L (2009) Imbalance between GABAergic and Glutamatergic Transmission Impairs Adult Neurogenesis in an Animal Model of Alzheimer's Disease. Cell stem cell 5 (6):624–633. doi:10.1016/j.stem.2009.10.003 [PubMed: 19951690]
3. Bie B, Wu J, Yang H, Xu JJ, Brown DL, Naguib M (2014) Epigenetic suppression of neuroligin 1 underlies amyloid-induced memory deficiency. Nat Neurosci 17 (2):223–231. doi:10.1038/nn.361810.1038/nn.3618http://www.nature.com/neuro/journal/vaop/ncurrent/abs/nn.3618.html#supplementaryinformationhttp://www.nature.com/neuro/journal/vaop/ncurrent/abs/nn.3618.html#supplementaryinformation [PubMed: 24441681]
4. Tremblay ME, Lowery RL, Majewska AK (2010) Microglial interactions with synapses are modulated by visual experience. PLoS Biol 8 (11):e1000527. doi:10.1371/journal.pbio.1000527 [PubMed: 21072242]
5. Tremblay ME, Majewska AK (2011) A role for microglia in synaptic plasticity? Commun Integr Biol 4 (2):220–222. doi:10.4161/cib.4.2.145061942-0889-4-2-22 [pii] [PubMed: 21655446]
6. Schafer DP, Lehrman EK, Kautzman AG, Koyama R, Mardinly AR, Yamasaki R, Ransohoff RM, Greenberg ME, Barres BA, Stevens B (2012) Microglia sculpt postnatal neural circuits in an activity and complement-dependent manner. Neuron 74 (4):691–705. doi:10.1016/j.neuron.2012.03.026 [PubMed: 22632727]
7. Schafer DP, Stevens B (2013) Phagocytic glial cells: sculpting synaptic circuits in the developing nervous system. Current opinion in neurobiology 23 (6):1034–1040. doi:10.1016/j.conb.2013.09.012 [PubMed: 24157239]
8. Paolicelli RC, Bolasco G, Pagani F, Maggi L, Scianni M, Panzanelli P, Giustetto M, Ferreira TA, Guiducci E, Dumas L, Ragozzino D, Gross CT (2011) Synaptic pruning by microglia is necessary for normal brain development. Science 333 (6048):1456–1458. doi:10.1126/science.1202529 [PubMed: 21778362]
9. Kettenmann H, Kirchhoff F, Verkhratsky A (2013) Microglia: new roles for the synaptic stripper. Neuron 77 (1):10–18. doi:10.1016/j.neuron.2012.12.023 [PubMed: 23312512]

10. Wake H, Moorhouse AJ, Miyamoto A, Nabekura J (2013) Microglia: actively surveying and shaping neuronal circuit structure and function. Trends in neurosciences 36 (4):209–217. doi: 10.1016/j.tins.2012.11.007 [PubMed: 23260014]

11. Hong S, Beja-Glasser VF, Nfonoyim BM, Frouin A, Li S, Ramakrishnan S, Merry KM, Shi Q, Rosenthal A, Barres BA, Lemere CA, Selkoe DJ, Stevens B (2016) Complement and microglia mediate early synapse loss in Alzheimer mouse models. Science. doi:10.1126/science.aad8373

12. Lui H, Zhang J, Makinson SR, Cahill MK, Kelley KW, Huang HY, Shang Y, Oldham MC, Martens LH, Gao F, Coppola G, Sloan SA, Hsieh CL, Kim CC, Bigio EH, Weintraub S, Mesulam MM, Rademakers R, Mackenzie IR, Seeley WW, Karydas A, Miller BL, Borroni B, Ghidoni R, Farese RV Jr., Paz JT, Barres BA, Huang EJ (2016) Progranulin Deficiency Promotes Circuit-Specific Synaptic Pruning by Microglia via Complement Activation. Cell 165 (4):921–935. doi:10.1016/j.cell.2016.04.001 [PubMed: 27114033]

13. Ricklin D, Hajishengallis G, Yang K, Lambris JD (2010) Complement: a key system for immune surveillance and homeostasis. Nature immunology 11 (9):785–797. doi:10.1038/ni.1923 [PubMed: 20720586]

14. Stephan AH, Barres BA, Stevens B (2012) The complement system: an unexpected role in synaptic pruning during development and disease. Annual review of neuroscience 35:369389. doi:10.1146/annurev-neuro-061010-113810

15. Bialas AR, Stevens B (2013) TGF-[beta] signaling regulates neuronal C1q expression and developmental synaptic refinement. Nat Neurosci 16 (12):1773–1782. doi:10.1038/nn.356010.1038/nn.3560http://www.nature.com/neuro/journal/v16/n12/abs/nn.3560.html#supplementary-informationhttp://www.nature.com/neuro/journal/v16/n12/abs/nn.3560.html#supplementary-information [PubMed: 24162655]

16. Ransohoff RM, Cardona AE (2010) The myeloid cells of the central nervous system parenchyma. Nature 468 (7321):253–262 [PubMed: 21068834]

17. Zhang J, Malik A, Choi HB, Ko RW, Dissing-Olesen L, Macvicar BA (2014) Microglial CR3 Activation Triggers Long-Term Synaptic Depression in the Hippocampus via NADPH Oxidase. Neuron 82 (1):195–207. doi:10.1016/j.neuron.2014.01.043 [PubMed: 24631344]

18. Stephan AH, Madison DV, Mateos JM, Fraser DA, Lovelett EA, Coutellier L, Kim L, Tsai HH, Huang EJ, Rowitch DH, Berns DS, Tenner AJ, Shamloo M, Barres BA (2013) A dramatic increase of C1q protein in the CNS during normal aging. The Journal of neuroscience : the official journal of the Society for Neuroscience 33 (33):13460–13474. doi:10.1523/JNEUROSCI.1333-13.2013

19. Wang DO, Martin KC, Zukin RS (2010) Spatially restricting gene expression by local translation at synapses. Trends in neurosciences 33 (4):173–182. doi:10.1016/j.tins.2010.01.005 [PubMed: 20303187]

20. Poon MM, Choi SH, Jamieson CA, Geschwind DH, Martin KC (2006) Identification of process-localized mRNAs from cultured rodent hippocampal neurons. The Journal of neuroscience : the official journal of the Society for Neuroscience 26 (51):13390–13399. doi:10.1523/JNEUROSCI.3432-06.2006 [PubMed: 17182790]

21. Wang DO, Kim SM, Zhao Y, Hwang H, Miura SK, Sossin WS, Martin KC (2009) Synapse- and stimulus-specific local translation during long-term neuronal plasticity. Science 324 (5934):1536–1540. doi:10.1126/science.1173205 [PubMed: 19443737]

22. Wu J, Bie B, Naguib M (2016) Epigenetic manipulation of brain-derived neurotrophic factor improves memory deficiency induced by neonatal anesthesia in rats. Anesthesiology 124 (3):624–640. doi:10.1097/aln.0000000000000981 [PubMed: 26649423]

23. Ashley CT Jr., Wilkinson KD, Reines D, Warren ST (1993) FMR1 protein: conserved RNP family domains and selective RNA binding. Science 262 (5133):563–566 [PubMed: 7692601]

24. Bassell GJ, Warren ST (2008) Fragile X syndrome: loss of local mRNA regulation alters synaptic development and function. Neuron 60 (2):201–214. doi:10.1016/j.neuron.2008.10.004 [PubMed: 18957214]

25. Hamilton A, Esseltine JL, DeVries RA, Cregan SP, Ferguson SS (2014) Metabotropic glutamate receptor 5 knockout reduces cognitive impairment and pathogenesis in a mouse model of Alzheimer's disease. Molecular brain 7:40. doi:10.1186/1756-6606-7-40 [PubMed: 24886239]

26. Aschrafi A, Cunningham BA, Edelman GM, Vanderklish PW (2005) The fragile X mental retardation protein and group I metabotropic glutamate receptors regulate levels of mRNA granules in brain. Proc Natl Acad Sci U S A 102 (6):2180–2185. doi:10.1073/pnas.0409803102 [PubMed: 15684045]
27. Di Prisco GV, Huang W, Buffington SA, Hsu CC, Bonnen PE, Placzek AN, Sidrauski C, Krnjevic K, Kaufman RJ, Walter P, Costa-Mattioli M (2014) Translational control of mGluRdependent long-term depression and object-place learning by eIF2alpha. Nat Neurosci 17 (8):1073–1082. doi: 10.1038/nn.3754 [PubMed: 24974795]
28. Ostapchenko VG, Beraldo FH, Guimaraes AL, Mishra S, Guzman M, Fan J, Martins VR, Prado VF, Prado MA (2013) Increased prion protein processing and expression of metabotropic glutamate receptor 1 in a mouse model of Alzheimer's disease. Journal of neurochemistry 127 (3): 415–425. doi:10.1111/jnc.12296 [PubMed: 23651058]
29. Chen X, Lin R, Chang L, Xu S, Wei X, Zhang J, Wang C, Anwyl R, Wang Q (2013) Enhancement of long-term depression by soluble amyloid beta protein in rat hippocampus is mediated by metabotropic glutamate receptor and involves activation of p38MAPK, STEP and caspase-3. Neuroscience 253:435–443. doi:10.1016/j.neuroscience.2013.08.054 [PubMed: 24012839]
30. Guan JS, Haggarty SJ, Giacometti E, Dannenberg JH, Joseph N, Gao J, Nieland TJ, Zhou Y, Wang X, Mazitschek R, Bradner JE, DePinho RA, Jaenisch R, Tsai LH (2009) HDAC2 negatively regulates memory formation and synaptic plasticity. Nature 459 (7243):55–60. doi:10.1038/ nature07925 [PubMed: 19424149]
31. Bie B, Zhang Z, Cai YQ, Zhu W, Zhang Y, Dai J, Lowenstein CJ, Weinman EJ, Pan ZZ (2010) Nerve growth factor-regulated emergence of functional delta-opioid receptors. The Journal of neuroscience : the official journal of the Society for Neuroscience 30 (16):56175628. doi: 30/16/5617 [pii] 10.1523/JNEUROSCI.5296-09.2010
32. Chacon MA, Barria MI, Soto C, Inestrosa NC (2004) Beta-sheet breaker peptide prevents Abeta-induced spatial memory impairments with partial reduction of amyloid deposits. Mol Psychiatry 9 (10):953–961. doi:10.1038/sj.mp.40015164001516 [pii] [PubMed: 15098004]
33. Paxinos G, Watson C (1998) The rat brain in stereotaxic coordinates. vol 1, 4th edition edn. Academic Press, New York
34. Bie B, Wu J, Foss JF, Naguib M (2018) Amyloid fibrils induce dysfunction of hippocampal glutamatergic silent synapses. Hippocampus 28 (8):549–556. doi:10.1002/hipo.22955 [PubMed: 29704282]
35. Wu J, Bie B, Yang H, Xu JJ, Brown DL, Naguib M (2013) Activation of the CB(2) receptor system reverses amyloid-induced memory deficiency. Neurobiology of aging 34:791–804. doi:10.1016/ j.neurobiolaging.2012.06.011 [PubMed: 22795792]
36. Wu J, Bie B, Yang H, Xu JJ, Brown DL, Naguib M (2013) Suppression of central chemokine fractalkine receptor signaling alleviates amyloid-induced memory deficiency. Neurobiology of aging 34 (12):2843–2852. doi:10.1016/j.neurobiolaging.2013.06.003 [PubMed: 23855980]
37. Yuede CM, Lee H, Restivo JL, Davis TA, Hettinger JC, Wallace CE, Young KL, Hayne MR, Bu G, Li CZ, Cirrito JR (2016) Rapid in vivo measurement of beta-amyloid reveals biphasic clearance kinetics in an Alzheimer's mouse model. J Exp Med 213 (5):677–685. doi:10.1084/jem.20151428 [PubMed: 27069115]
38. Janssen L, Keppens C, De Deyn PP, Van Dam D (2016) Late age increase in soluble amyloid-beta levels in the APP23 mouse model despite steady-state levels of amyloid-betaproducing proteins. Biochim Biophys Acta 1862 (1):105–112. doi:10.1016/j.bbadis.2015.10.027 [PubMed: 26542217]
39. Schieb H, Kratzin H, Jahn O, Mobius W, Rabe S, Staufenbiel M, Wiltfang J, Klafki HW (2011) Beta-amyloid peptide variants in brains and cerebrospinal fluid from amyloid precursor protein (APP) transgenic mice: comparison with human Alzheimer amyloid. J Biol Chem 286 (39): 33747–33758. doi:10.1074/jbc.M111.246561 [PubMed: 21795681]
40. Shin RW, Ogino K, Kondo A, Saido TC, Trojanowski JQ, Kitamoto T, Tateishi J (1997) Amyloid beta-protein (Abeta) 1–40 but not Abeta1–42 contributes to the experimental formation of Alzheimer disease amyloid fibrils in rat brain. Journal of Neuroscience 17 (21):8187–8193 [PubMed: 9334394]

41. Ahmed T, Enam SA, Gilani AH (2010) Curcuminoids enhance memory in an amyloidinfused rat model of Alzheimer's disease. Neuroscience 169 (3):1296–1306. doi:S03064522(10)00818–3 [pii] 10.1016/j.neuroscience.2010.05.078 [PubMed: 20538041]

42. Bie B, Zhu W, Pan ZZ (2009) Ethanol-induced delta-opioid receptor modulation of glutamate synaptic transmission and conditioned place preference in central amygdala. Neuroscience 160 (2): 348–358. doi:S0306–4522(09)00262–0 [pii] 10.1016/j.neuroscience.2009.02.049 [PubMed: 19258026]

43. Maphis N, Xu G, Kokiko-Cochran ON, Jiang S, Cardona A, Ransohoff RM, Lamb BT, Bhaskar K (2015) Reactive microglia drive tau pathology and contribute to the spreading of pathological tau in the brain. Brain 138 (Pt 6):1738–1755. doi:10.1093/brain/awv081 [PubMed: 25833819]

44. Wu J, Hocevar M, Foss JF, Bihua Bie B, Naguib M (2017) Activation of CB2 receptor system restores cognitive capacity and hippocampal Sox2 expression in a transgenic mouse model of Alzheimer's disease. European journal of pharmacology 811:12–20. doi:10.1016/j.ejphar.2017.05.044 [PubMed: 28551012]

45. Bie B, Brown DL, Naguib M (2011) Increased synaptic GluR1 subunits in the anterior cingulate cortex of rats with peripheral inflammation. European journal of pharmacology 653 (1–3):26–31. doi:S0014–2999(10)01197–0 [pii] 10.1016/j.ejphar.2010.11.027 [PubMed: 21147092]

46. Peritz T, Zeng F, Kannanayakal TJ, Kilk K, Eiriksdottir E, Langel U, Eberwine J (2006) Immunoprecipitation of mRNA-protein complexes. Nat Protoc 1 (2):577–580. doi:10.1038/nprot.2006.82 [PubMed: 17406284]

47. Bie B, Peng Y, Zhang Y, Pan ZZ (2005) cAMP-mediated mechanisms for pain sensitization during opioid withdrawal. The Journal of neuroscience : the official journal of the Society for Neuroscience 25 (15):3824–3832. doi:25/15/3824 [pii] 10.1523/JNEUROSCI.5010-04.2005

48. Zhang M, Wang Q, Huang Y (2007) Fragile X mental retardation protein FMRP and the RNA export factor NXF2 associate with and destabilize Nxf1 mRNA in neuronal cells. Proc Natl Acad Sci U S A 104 (24):10057–10062. doi:10.1073/pnas.0700169104 [PubMed: 17548835]

49. Li Y, Stockton ME, Bhuiyan I, Eisinger BE, Gao Y, Miller JL, Bhattacharyya A, Zhao X (2016) MDM2 inhibition rescues neurogenic and cognitive deficits in a mouse model of fragile X syndrome. Sci Transl Med 8 (336):336ra361. doi:10.1126/scitranslmed.aad9370

50. Bie B, Zhu W, Pan ZZ (2009) Rewarding morphine-induced synaptic function of delta-opioid receptors on central glutamate synapses. J Pharmacol Exp Ther 329 (1):290–296. doi:jpet.108.148908 [pii] 10.1124/jpet.108.148908 [PubMed: 19168708]

51. Michailidou I, Willems JG, Kooi EJ, van Eden C, Gold SM, Geurts JJ, Baas F, Huitinga I, Ramaglia V (2015) Complement C1q-C3-associated synaptic changes in multiple sclerosis hippocampus. Ann Neurol 77 (6):1007–1026. doi:10.1002/ana.24398 [PubMed: 25727254]

52. Perry VH, Nicoll JAR, Holmes C (2010) Microglia in neurodegenerative disease. Nat Rev Neurol 6 (4):193–201 [PubMed: 20234358]

53. Zhan Y, Paolicelli RC, Sforazzini F, Weinhard L, Bolasco G, Pagani F, Vyssotski AL, Bifone A, Gozzi A, Ragozzino D, Gross CT (2014) Deficient neuron-microglia signaling results in impaired functional brain connectivity and social behavior. Nat Neurosci 17 (3):400–406. doi:10.1038/nn.3641 [PubMed: 24487234]

54. Wake H, Moorhouse AJ, Jinno S, Kohsaka S, Nabekura J (2009) Resting microglia directly monitor the functional state of synapses in vivo and determine the fate of ischemic terminals. The Journal of neuroscience : the official journal of the Society for Neuroscience 29 (13):3974–3980. doi:10.1523/JNEUROSCI.4363-08.2009 [PubMed: 19339593]

55. Brown GC, Neher JJ (2014) Microglial phagocytosis of live neurons. Nature reviews Neuroscience 15 (4):209–216. doi:10.1038/nrn3710 [PubMed: 24646669]

56. Fuhrmann M, Bittner T, Jung CK, Burgold S, Page RM, Mitteregger G, Haass C, LaFerla FM, Kretzschmar H, Herms J (2010) Microglial Cx3cr1 knockout prevents neuron loss in a mouse model of Alzheimer's disease. Nature neuroscience 13 (4):411–413. doi:10.1038/nn.2511 [PubMed: 20305648]

57. Kokiko-Cochran O, Ransohoff L, Veenstra M, Lee S, Saber M, Sikora M, Teknipp R, Xu G, Bemiller S, Wilson G, Crish S, Bhaskar K, Lee YS, Ransohoff RM, Lamb BT (2016) Altered

Neuroinflammation and Behavior after Traumatic Brain Injury in a Mouse Model of Alzheimer's Disease. J Neurotrauma 33 (7):625–640. doi:10.1089/neu.2015.3970 [PubMed: 26414955]

58. Webster SJ, Van Eldik LJ, Watterson DM, Bachstetter AD (2015) Closed head injury in an age-related Alzheimer mouse model leads to an altered neuroinflammatory response and persistent cognitive impairment. The Journal of neuroscience : the official journal of the Society for Neuroscience 35 (16):6554–6569. doi:10.1523/JNEUROSCI.0291-15.2015
59. Lalonde R, Kim HD, Maxwell JA, Fukuchi K (2005) Exploratory activity and spatial learning in 12-month-old APP(695)SWE/co+PS1/DeltaE9 mice with amyloid plaques. Neurosci Lett 390 (2): 87–92. doi:10.1016/j.neulet.2005.08.028 [PubMed: 16169151]
60. Volianskis A, Kostner R, Molgaard M, Hass S, Jensen MS (2010) Episodic memory deficits are not related to altered glutamatergic synaptic transmission and plasticity in the CA1 hippocampus of the APPswe/PS1deltaE9-deleted transgenic mice model of ss-amyloidosis. Neurobiology of aging 31 (7):1173–1187. doi:10.1016/j.neurobiolaging.2008.08.005 [PubMed: 18790549]
61. Holcomb L, Gordon MN, McGowan E, Yu X, Benkovic S, Jantzen P, Wright K, Saad I, Mueller R, Morgan D, Sanders S, Zehr C, O'Campo K, Hardy J, Prada CM, Eckman C, Younkin S, Hsiao K, Duff K (1998) Accelerated Alzheimer-type phenotype in transgenic mice carrying both mutant amyloid precursor protein and presenilin 1 transgenes. Nat Med 4 (1):97–100 [PubMed: 9427614]
62. Gong B, Vitolo OV, Trinchese F, Liu S, Shelanski M, Arancio O (2004) Persistent improvement in synaptic and cognitive functions in an Alzheimer mouse model after rolipram treatment. J Clin Invest 114 (11):1624–1634. doi:10.1172/JCI22831 [PubMed: 15578094]
63. Montarolo F, Parolisi R, Hoxha E, Boda E, Tempia F (2013) Early enriched environment exposure protects spatial memory and accelerates amyloid plaque formation in APP(Swe)/PS1(L166P) mice. PLoS One 8 (7):e69381. doi:10.1371/journal.pone.0069381 [PubMed: 23894463]
64. Viana da Silva S, Haberl MG, Zhang P, Bethge P, Lemos C, Goncalves N, Gorlewicz A, Malezieux M, Goncalves FQ, Grosjean N, Blanchet C, Frick A, Nagerl UV, Cunha RA, Mulle C (2016) Early synaptic deficits in the APP/PS1 mouse model of Alzheimer's disease involve neuronal adenosine A2A receptors. Nat Commun 7:11915. doi:10.1038/ncomms11915 [PubMed: 27312972]
65. Stevens B, Allen NJ, Vazquez LE, Howell GR, Christopherson KS, Nouri N, Micheva KD, Mehalow AK, Huberman AD, Stafford B, Sher A, Litke AM, Lambris JD, Smith SJ, John SW, Barres BA (2007) The classical complement cascade mediates CNS synapse elimination. Cell 131 (6):1164–1178. doi:10.1016/j.cell.2007.10.036 [PubMed: 18083105]
66. Takano M, Kawabata S, Komaki Y, Shibata S, Hikishima K, Toyama Y, Okano H, Nakamura M (2014) Inflammatory cascades mediate synapse elimination in spinal cord compression. Journal of neuroinflammation 11:40. doi:10.1186/1742-2094-11-40 [PubMed: 24589419]
67. Zhang Z, Pinto AM, Wan L, Wang W, Berg MG, Oliva I, Singh LN, Dengler C, Wei Z, Dreyfuss G (2013) Dysregulation of synaptogenesis genes antecedes motor neuron pathology in spinal muscular atrophy. Proc Natl Acad Sci U S A 110 (48):19348–19353. doi:10.1073/pnas.1319280110 [PubMed: 24191055]
68. Chu Y, Jin X, Parada I, Pesic A, Stevens B, Barres B, Prince DA (2010) Enhanced synaptic connectivity and epilepsy in C1q knockout mice. Proc Natl Acad Sci U S A 107 (17):79757980. doi:10.1073/pnas.0913449107
69. Shen Y, Li R, McGeer EG, McGeer PL (1997) Neuronal expression of mRNAs for complement proteins of the classical pathway in Alzheimer brain. Brain Res 769 (2):391395
70. Fischer B, Schmoll H, Riederer P, Bauer J, Platt D, Popa-Wagner A (1995) Complement C1q and C3 mRNA expression in the frontal cortex of Alzheimer's patients. J Mol Med (Berl) 73 (9):465–471 [PubMed: 8528750]
71. Matsuda K, Budisantoso T, Mitakidis N, Sugaya Y, Miura E, Kakegawa W, Yamasaki M, Konno K, Uchigashima M, Abe M, Watanabe I, Kano M, Watanabe M, Sakimura K, Aricescu AR, Yuzaki M (2016) Transsynaptic Modulation of Kainate Receptor Functions by C1q-like Proteins. Neuron 90 (4):752–767. doi:10.1016/j.neuron.2016.04.001 [PubMed: 27133466]
72. Rostami E, Davidsson J, Gyorgy A, Agoston DV, Risling M, Bellander BM (2013) The terminal pathway of the complement system is activated in focal penetrating but not in mild diffuse traumatic brain injury. J Neurotrauma 30 (23):1954–1965. doi:10.1089/neu.2012.2583 [PubMed: 23808389]

73. Schafer MK, Schwaeble WJ, Post C, Salvati P, Calabresi M, Sim RB, Petry F, Loos M, Weihe E (2000) Complement C1q is dramatically up-regulated in brain microglia in response to transient global cerebral ischemia. J Immunol 164 (10):5446–5452 [PubMed: 10799911]
74. Zipfel PF, Skerka C (2009) Complement regulators and inhibitory proteins. Nat Rev Immunol 9 (10):729–740. doi:10.1038/nri2620 [PubMed: 19730437]
75. Ceman S, O'Donnell WT, Reed M, Patton S, Pohl J, Warren ST (2003) Phosphorylation influences the translation state of FMRP-associated polyribosomes. Human molecular genetics 12 (24):3295–3305. doi:10.1093/hmg/ddg350 [PubMed: 14570712]
76. Martin HGS, Lassalle O, Brown JT, Manzoni OJ (2016) Age-Dependent Long-Term Potentiation Deficits in the Prefrontal Cortex of the Fmr1 Knockout Mouse Model of Fragile X Syndrome. Cereb Cortex 26 (5):2084–2092. doi:10.1093/cercor/bhv031 [PubMed: 25750254]
77. Sokol DK, Maloney B, Long JM, Ray B, Lahiri DK (2011) Autism, Alzheimer disease, and fragile X: APP, FMRP, and mGluR5 are molecular links. Neurology 76 (15):1344–1352. doi:10.1212/WNL.0b013e3182166dc7 [PubMed: 21482951]
78. Lee EK, Kim HH, Kuwano Y, Abdelmohsen K, Srikantan S, Subaran SS, Gleichmann M, Mughal MR, Martindale JL, Yang X, Worley PF, Mattson MP, Gorospe M (2010) hnRNP C promotes APP translation by competing with FMRP for APP mRNA recruitment to P bodies. Nature structural & molecular biology 17 (6):732–739. doi:10.1038/nsmb.1815
79. Ronesi JA, Huber KM (2008) Metabotropic glutamate receptors and fragile x mental retardation protein: partners in translational regulation at the synapse. Science signaling 1 (5):pe6. doi:10.1126/stke.15pe6 [PubMed: 18272470]
80. Kim SH, Steele JW, Lee SW, Clemenson GD, Carter TA, Treuner K, Gadient R, Wedel P, Glabe C, Barlow C, Ehrlich ME, Gage FH, Gandy S (2014) Proneurogenic Group II mGluR antagonist improves learning and reduces anxiety in Alzheimer Abeta oligomer mouse. Mol Psychiatry. doi:10.1038/mp.2014.87
81. Lavreysen H, Wouters R, Bischoff F, Nobrega Pereira S, Langlois X, Blokland S, Somers M, Dillen L, Lesage AS (2004) JNJ16259685, a highly potent, selective and systemically active mGlu1 receptor antagonist. Neuropharmacology 47 (7):961–972. doi:10.1016/j.neuropharm.2004.08.007 [PubMed: 15555631]
82. Niswender CM, Conn PJ (2010) Metabotropic glutamate receptors: physiology, pharmacology, and disease. Annu Rev Pharmacol Toxicol 50:295–322. doi:10.1146/annurev.pharmtox.011008.145533 [PubMed: 20055706]

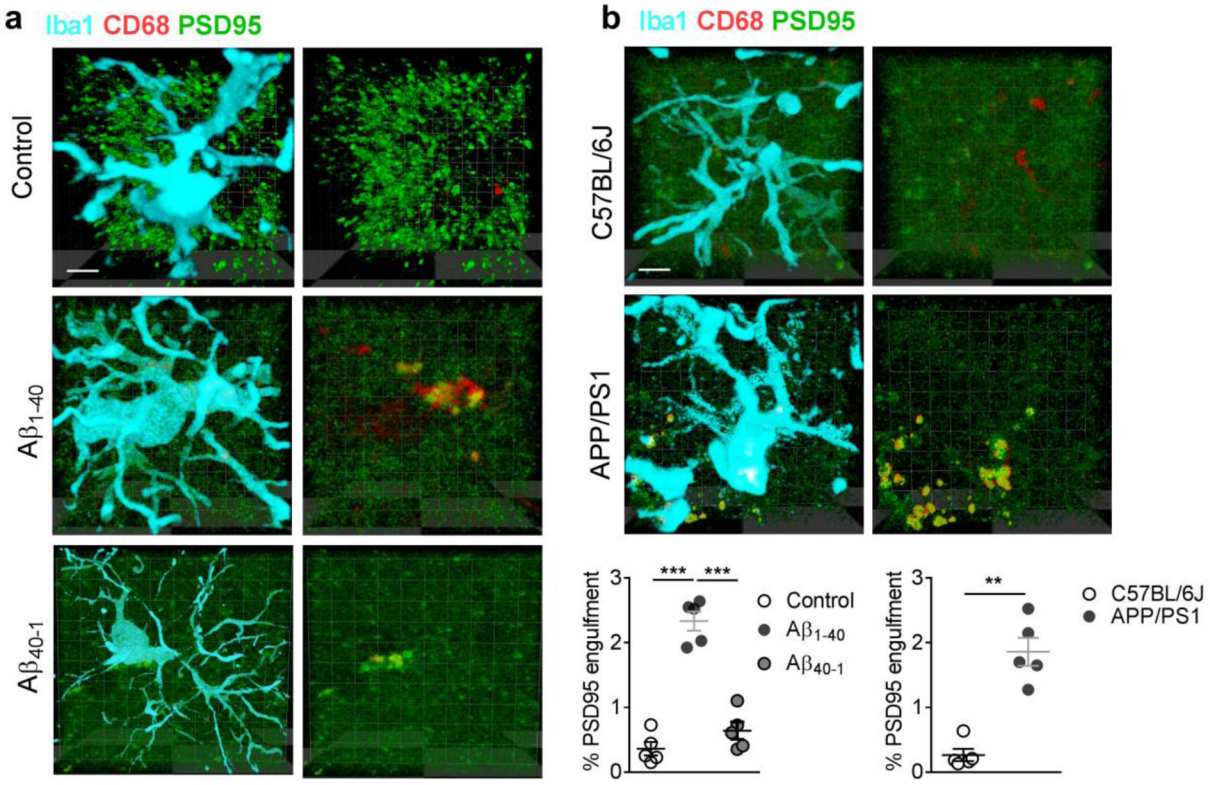

Figure 1. Hippocampal injection of $A\beta_{1–40}$ fibrils impaired memory, decreased glutamatergic transmission, and induced microglia activation.

Significantly extended escape latency (**a,** n = 10 rats in each group, effect of group [$F_{2,27}$ = 20.3, P<0.0001], effect of time [$F_{4,27}$ = 180.1, P<0.0001], interaction between group and time [P= 0.25]) and (**b**) less time spent in the target quadrant (T, target quadrant; R, right quadrant; O, opposite quadrant; L, left quadrant) (**b,** n = 10 rats in each group, $F_{2,27}$ = 8.71, P = 0.001) were observed in the rats microinjected with $A\beta_{1–40}$ fibrils, but not $A\beta_{40–1}$ fibrils nor artificial CSF. (**b**) Representative path tracings in each quadrant during the probe trial on day 6 (T, target quadrant; R, right quadrant; O, opposite quadrant; L, left quadrant). Significantly attenuated input (stimulus intensity) - output (EPSC amplitude) response of evoked EPSCs was also observed in the hippocampal CA1 neurons of the rats injected with amyloid fibrils (**c**, n = 14 neurons in each group, $F_{2,39}$ = 21.8, P<0.0001). The amplitude (**d**, n = 12 rats in each group, unpaired t-test, t = 5.93, DF = 22, two-tailed P<0.0001) and inter-event interval (**d**, n = 12 rats in each group, unpaired t-test, t =3.33, DF = 22, two-tailed P = 0.003) of mEPSC were altered in the rats injected with amyloid fibrils. Increased Iba1 intensity of microglia processes were observed in the hippocampal CA1 of the rats injected with amyloid fibrils (**e**, n = 5 rats in each group, t = 4.7, DF = 8, two-tailed P = 0.0015, scale bar = 40 μm). Iba1 intensity was calculated as following: Intensity = area × average of immunosignal (filtered out of the noise signal). Increased immunosignal of CD68 (red) was observed in microglia (Iba1, cyan) in the rats injected with amyloid fibrils. The ratio between the volume of CD68-positive and Iba-positive immunosignals in 3D images was presented. (**f**, n = 5 rats in each group, t = 11.4, DF = 8, two-tailed P <0.001, scale bar = 10 μm). Right micrographs were presented to show the same microglia in which only the

lysosomes (red) was visualized. Each dot represents the mean value of 4 brain sections of one animal. Data represent mean ± s.e.m. For box-and-whiskers plots, the box extends from the 25th to 75th percentiles, a line within the box marks the median. Whiskers (error bars) above and below the box represent the minimum and maximum values. *P<0.05, **P<0.01, ***P<0.001.

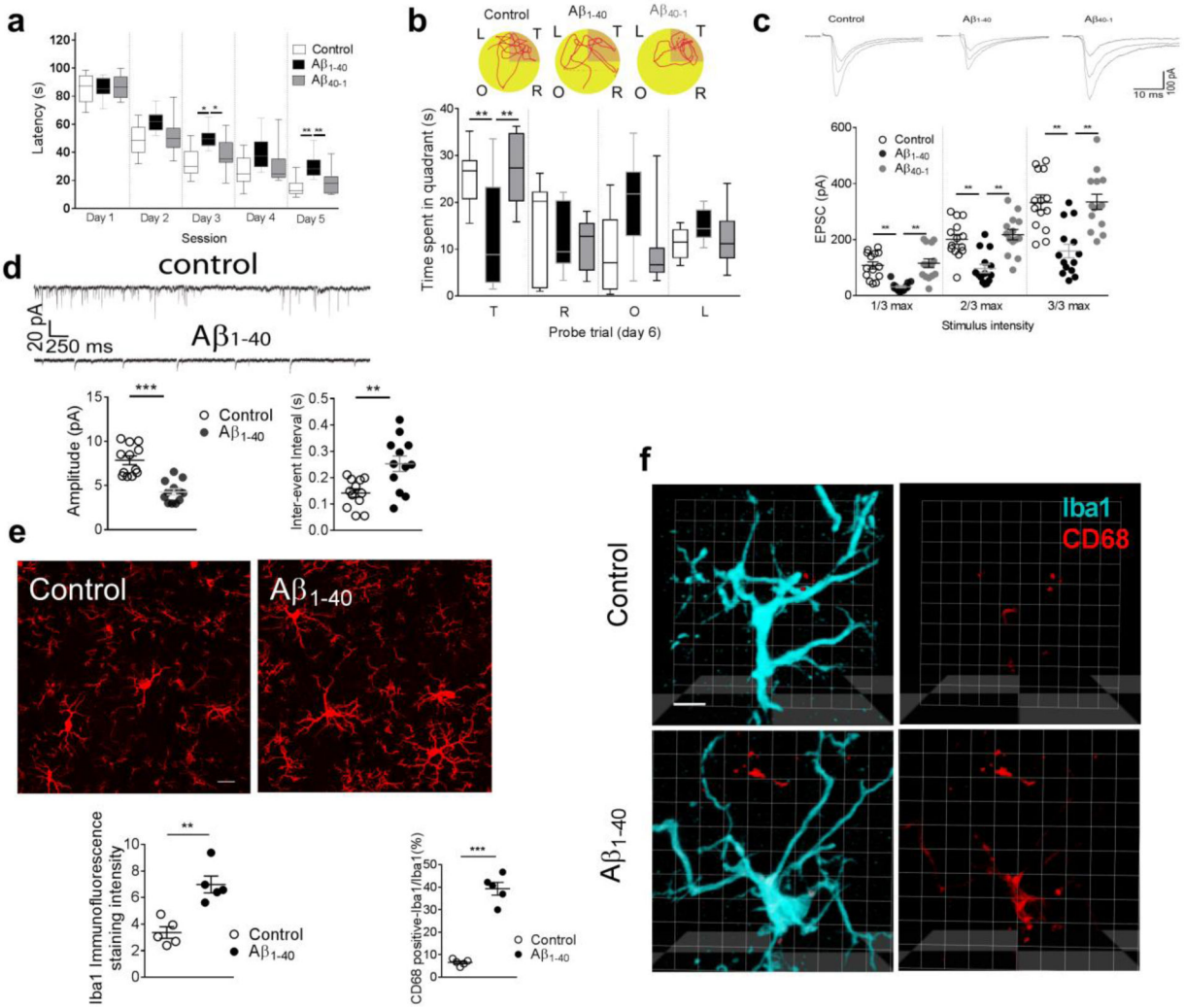

Figure 2. Increased microglial phagocytosis of glutamatergic synapses in rodent AD model.

Increased internalization of postsynaptic marker PSD95 was observed in the lysosomes (CD68) within the microglia (Iba1) in the rats injected with $A\beta_{1–40}$ fibrils, but not those injected with $A\beta_{40–1}$ fibrils (***a***, n = 5 rats in each group, $F_{2,12} = 67.6$, P<0.0001, scale bar = 10 μm). A micrograph was presented at the right to show the same microglia in which only the lysosomes (red) and PSD95 (green) were visualized. Similar increases in co-localization of PSD95 with lysosome marker CD68 within the microglia were observed in the hippocampal CA1 of the Tg-APPsw/PSEN1DE9 (APP/PSI) mice (***b***, n = 5 mice in each group, Mann-Whitney U-statistic <0.0001, two-tailed P = 0.008, scale bar = 10 μm). Data represent mean ± s.e.m. Each dot represents the mean value of 4 brain sections of one animal. **P<0.01, ***P<0.001.

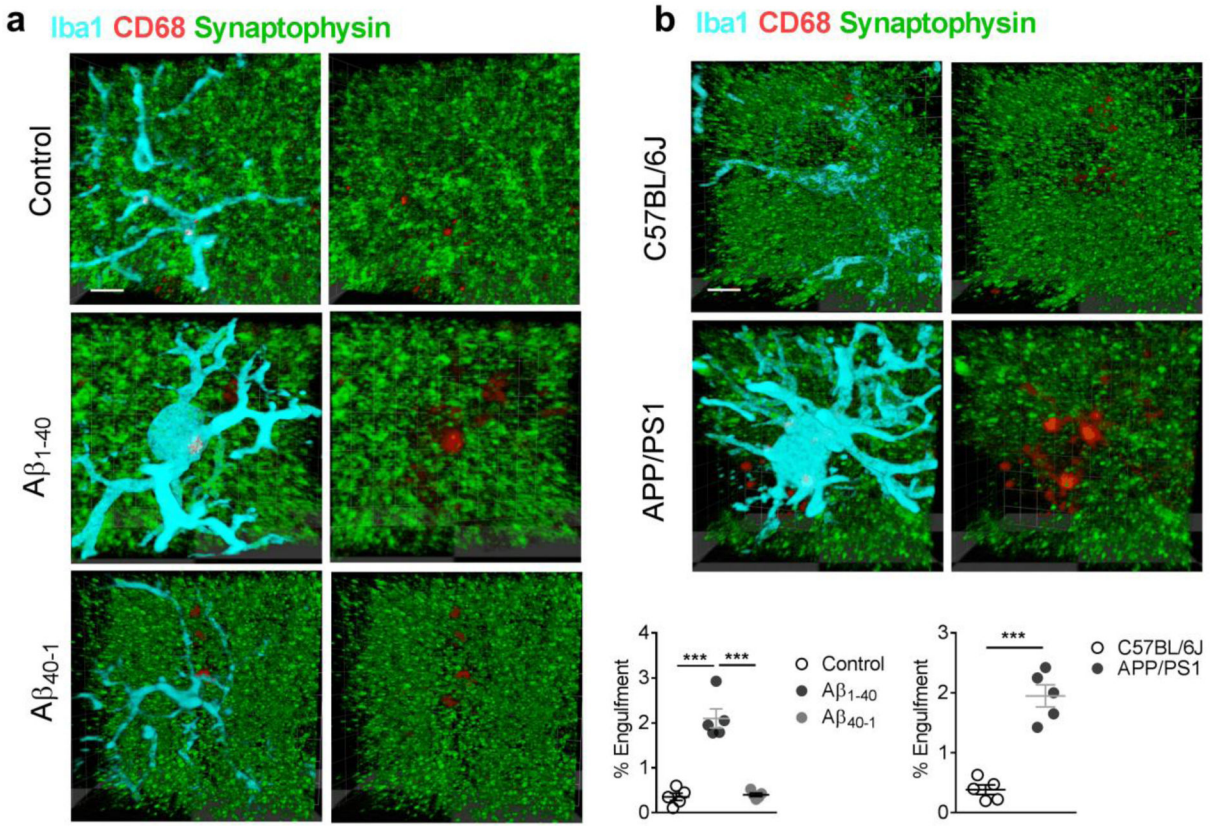

Figure 3.

Increased internalization of presynaptic marker synaptophysin was observed in the lysosomes (CD68) within the microglia (Iba1) in the rats injected with $A\beta_{1–40}$ fibrils, but not those injected with $A\beta_{40–1}$ fibrils (***a***, n = 5 rats in each group, $F_{2,13} = 55.2$, P <0.0001, scale bar = 10 μm). A micrograph was presented at the right to show the same microglia (Iba1-positive, cyan) in which only the lysosomes (red) and synaptophysin (green) were visualized. Similar increases in co-localization of synaptophysin with lysosome marker CD68 within the microglia were observed in the hippocampal CA1 of the Tg-APPsw/PSEN1DE9 (APP/PSI) mice (***b***, n = 5 mice in each group, unpaired t-test, t = 7.8, DF = 8, two-tailed P <0.0001, scale bar = 10 μm). Each dot represents the mean value of 4 brain sections of one animal. Data represent mean ± s.e.m. ***P<0.001.

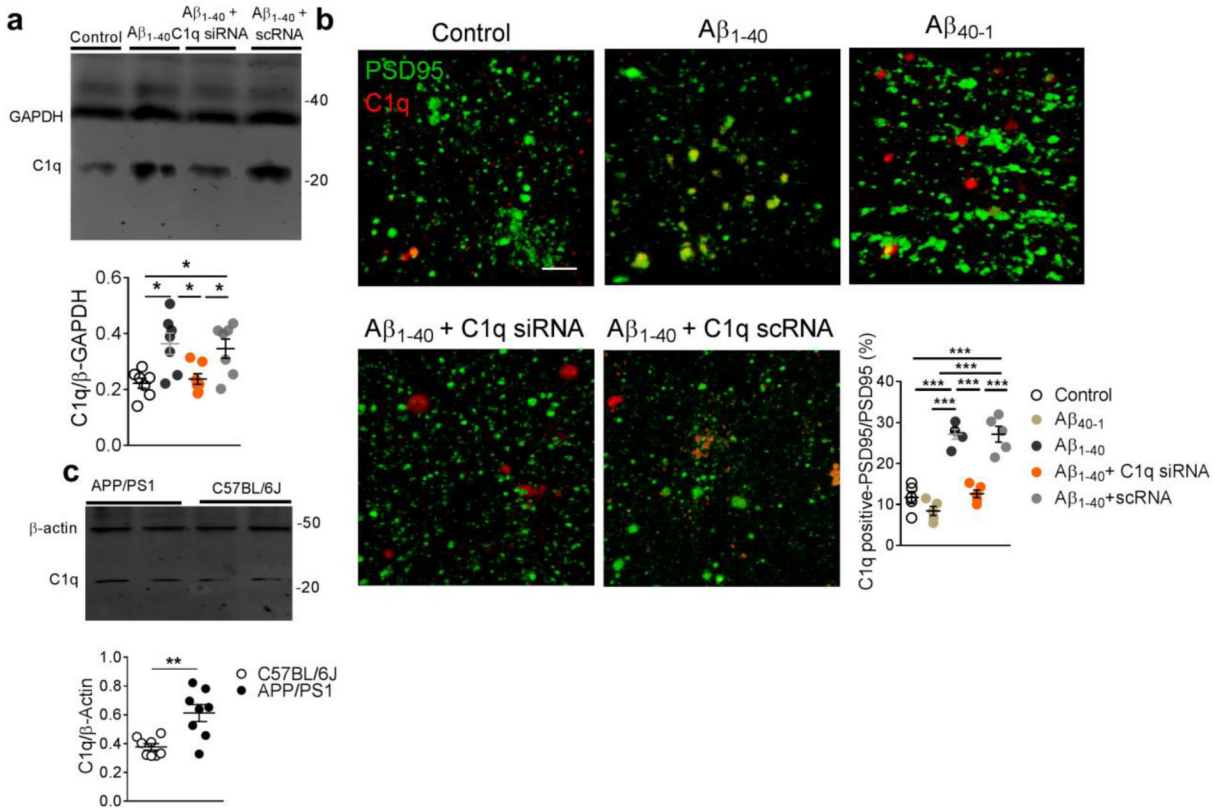

Figure 4. Increased C1q distribution in the glutamatergic synapse.

Significantly increased C1q expression was observed in the hippocampal synaptosomal preparation of the rats injected with amyloid fibrils, which was effectively attenuated by C1q siRNA (***a***, n = 7 rats in each group, $F_{3,24}$ = 6.3, P = 0.0026). Significantly increased co-localization of C1q with PSD95 was observed in the hippocampal CA1 of the rats injected with $A\beta_{1–40}$ fibrils, but not those injected with $A\beta_{40–1}$ fibrils (***b***, n = 5 rats in each group, $F_{4,20}$ = 42.8, P <0.0001, scale bar = 10 μm). Each dot represents the mean value of 4 brain sections of one animal. Significantly increased expression of C1q was observed in hippocampal CA1 synaptosomal preparation in the Tg-APPsw/PSEN1DE9 (APP/PSI) compared to C57BL/6 mice (***c***, n = 8 mice in each group, unpaired t-test, t = 3.7, DF = 14, two-tailed P = 0.002). Data represent mean ± s.e.m. *P<0.05, **P<0.01, ***P<0.001.

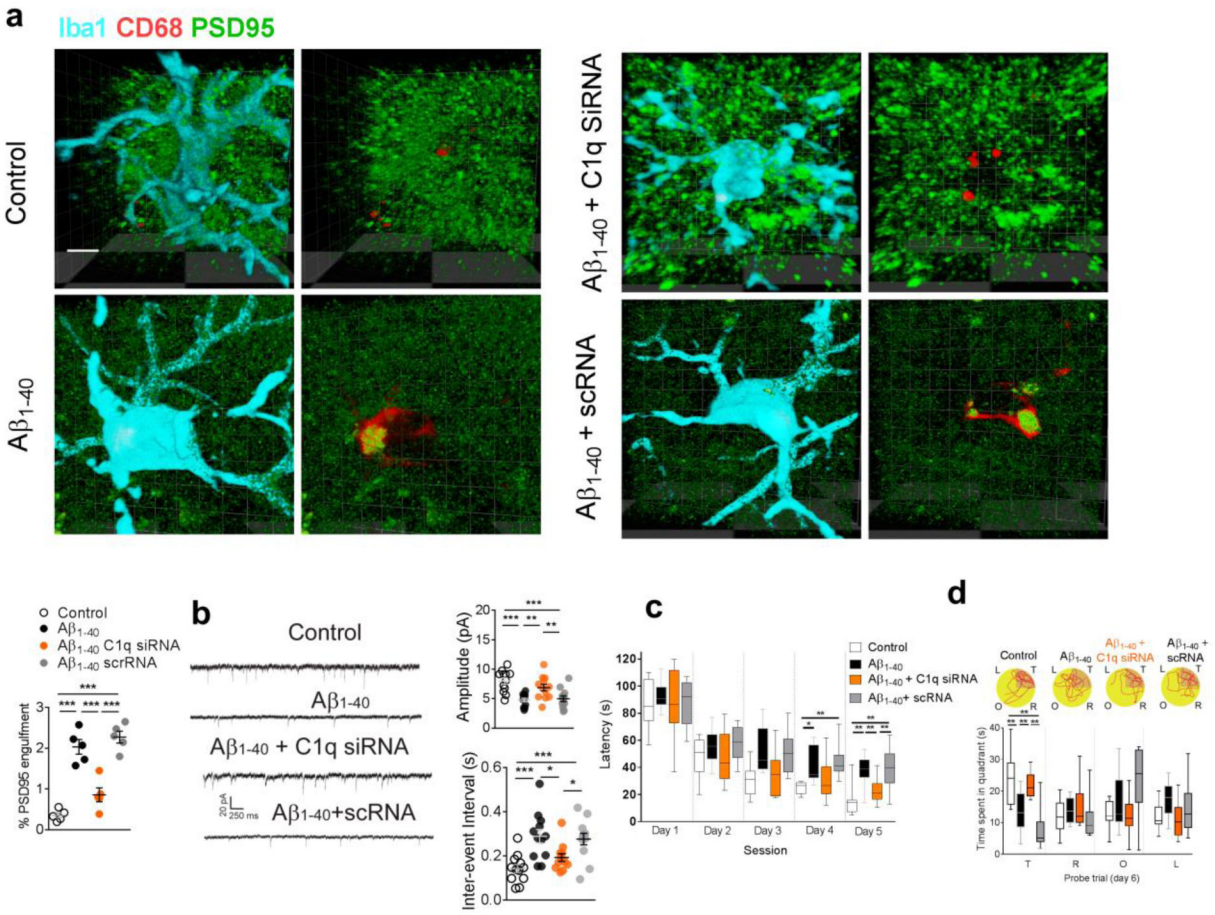

Figure 5. Suppression of C1q attenuated the microglial phagocytosis of glutamatergic synapse induced by amyloid fibrils.

C1q siRNA significantly decreased the internalization of PSD95 in lysosomes (CD68) within microglia in the rats injected with amyloid fibrils (***a***, n = 5 rats in each group, $F_{3,16}$ = 39.6, P<0.0001, scale bar = 10 μm). Each dot represents the mean value of 4 brain sections of one animal. C1q siRNA significantly recovered the amplitude (***b***, n = 12 rats in each group, $F_{3,44}$ = 10.33, P<0.0001) and inter-events interval (***b***, n = 12 rats in each group, $F_{3,44}$ = 8.5, P = 0.0001) of mEPSCs in the hippocampal CA1 neurons in the rats injected with amyloid fibrils. C1q siRNA microinjection also shortened the escape latency (***c***, n = 10 rats in each group, effect of group [$F_{3,36}$ = 11.4, P<0.0001], effect of time [$F_{4,36}$ = 108.8, P<0.0001], interaction between group and time [P = 0.37]) and increased the time spent in the target quadrant in the amyloid-injected rats (***d***, n = 10 rats in each group, $F_{3,36}$ = 13.9, P<0.0001). (***d***) Representative path tracings in each quadrant during the probe trial on day 6 (T, target quadrant; R, right quadrant; O, opposite quadrant; L, left quadrant). Data represent mean ± s.e.m. For box-and-whiskers plots, the box extends from the 25th to 75th percentiles, a line within the box marks the median. Whiskers (error bars) above and below the box represent the minimum and maximum values. *P<0.05, **P<0.01, ***P<0.001.

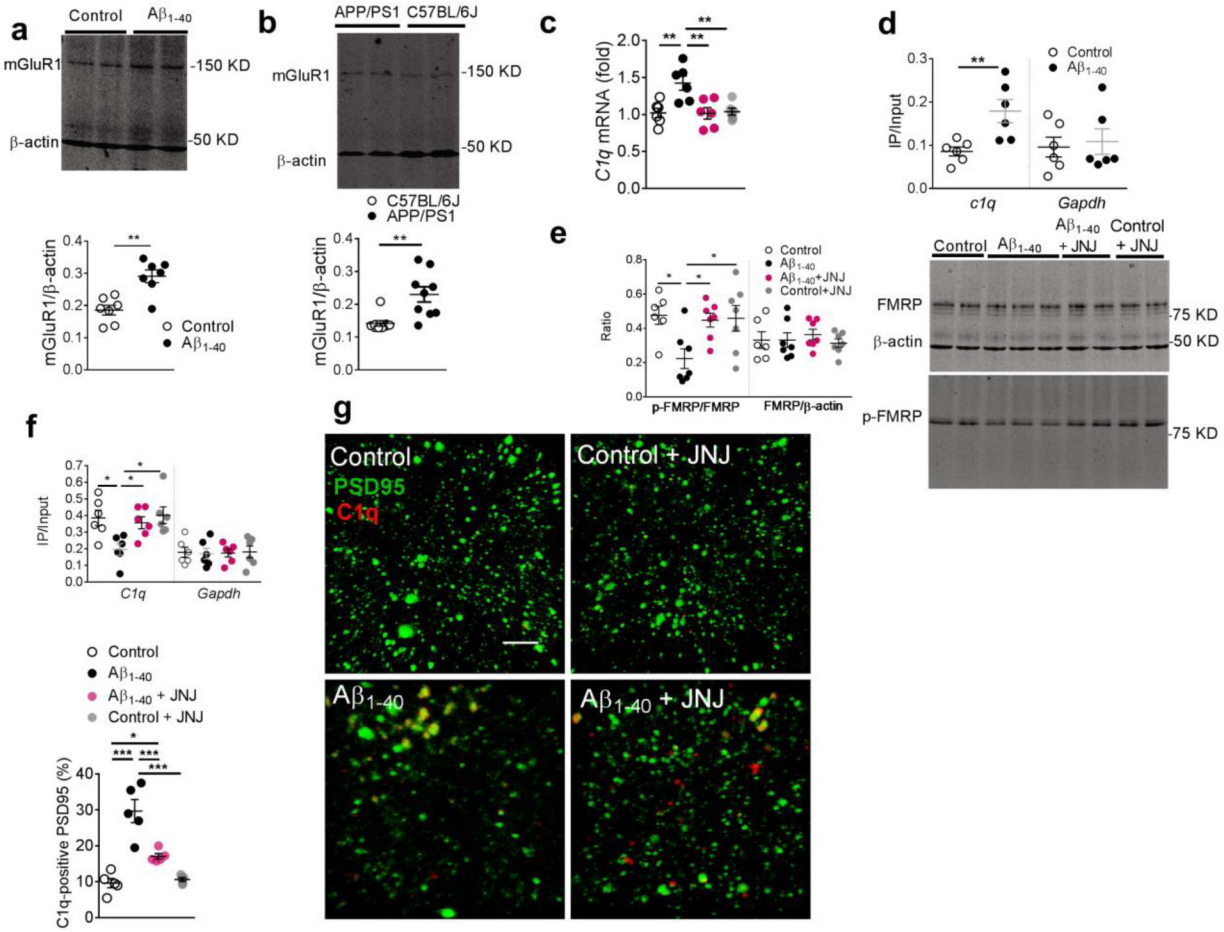

Figure 6. Inhibition of metabotropic glutamate receptor 1 (mGluR1) signaling attenuated the C1q upregulation induced by amyloid fibrils.

Significantly increased expression of mGluR1 was observed in the hippocampal CA1 in the rats injected with amyloid fibrils (***a***, n = 7 rats in each group, unpaired t-test, t = 4.3, DF = 12, two-tailed P = 0.001) and Tg-APPsw/PSEN1DE9 (APP/PSI) mice (***b***, n = 9 mice in each group, unpaired t-test, t = 3.6, DF = 16, two-tailed P = 0.003). Significantly increased *C1q* mRNA was detected in the hippocampal synaptosomal preparation in the modeled rats, which was attenuated by JNJ16259685 (***c***, n = 6 rats in each group, $F_{3,20}$ = 7.46, P = 0.002). Increased C1q mRNA was pulled by e-IF4E antibody in hippocampal CA1 lysates of the rats injected with amyloid fibrils (***d***, n = 6 rats per group, t = 3.3, DF = 10, two-tailed P = 0.009). Amyloid fibrils decreased the phosphorylation of fragile X mental retardation protein (FMRP) in the hippocampal CA1, which was recovered by the mGluR1 inhibitor JNJ16259685 (***e***, n = 6,7,7,7 rats, $F_{3,23}$ = 4.3, P = 0.015); (**f**) RNA-IP study revealed a significantly decreased amount of C1q mRNA pulled-down by p-FMRP antibody in the hippocampal CA1 in the modeled rats, which was recovered by JNJ16259685 (***f***, n = 6 rats in each group, $F_{3,20}$ = 4.97, P = 0.009). Microinjection of JNJ16259685 significantly decreased C1q immunosignals co-localized with the PSD95 in the hippocampal CA1 in the amyloidinjected rats (***g***, n = 5 rats in each group, $F_{3,16}$ = 26.5, P <0.0001, scale bar = 10 μm). Each dot represents the mean value of 4 brain sections of one rat. Data represent mean ± s.e.m. *P<0.05, **P<0.01, ***P<0.001.

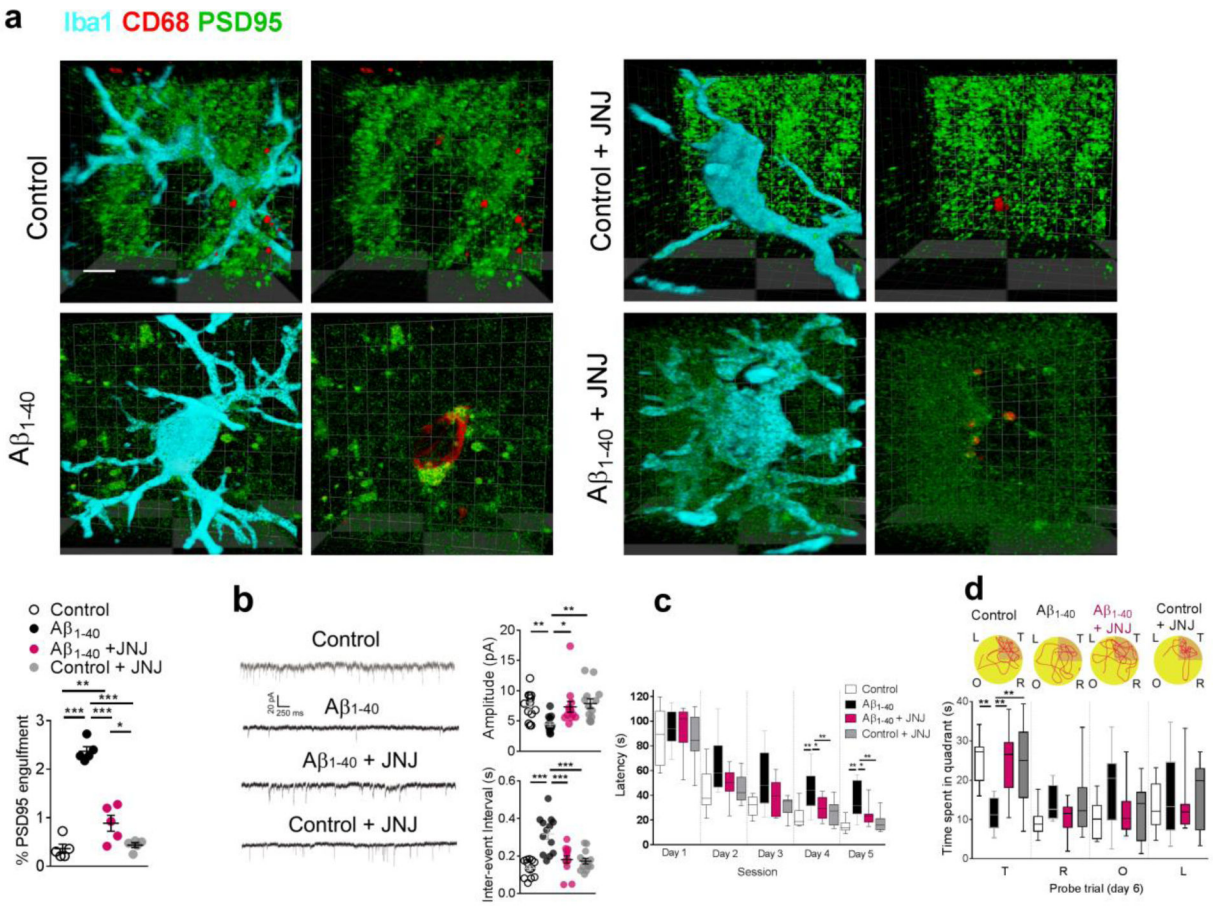

Figure 7. Inhibition of mGluR1 signaling attenuated the microglia phagocytosis of synapses induced by amyloid fibrils.

JNJ16259685 significantly decreased the internalization of PSD95 with lysosome marker CD68 in microglia (Iba1) in the rats injected with amyloid fibrils (***a***, n = 5 rats in each group, $F_{3,16}$ = 73.0, P <0.0001, scale bar = 10 μm). Each dot represents the mean value of 4 brain sections of one animal. Microinjection of JNJ16259685 significantly recovered the amplitude (***b***, n = 13 rats in each group, Kruskal-Wallis Statistic KW = 18.2, P = 0.0004) and inter-event interval of mEPSCs (***b***, n = 13 rats in each group, $F_{3,48}$ = 16.8, P<0.0001) in the hippocampal CA1 neurons in the rats injected with amyloid fibrils. Microinjection of JNJ16259685 also shortened the escape latency (***c,*** n = 10 rats in each group, effect of group [$F_{3,36}$ = 13.3, P<0.0001], effect of time [$F_{4,36}$ = 135.5, P<0.0001], interaction between group and time [P = 0.47]) and increased the time spent in the target quadrant (***d,*** n = 10 rats in each group, $F_{4,36}$ = 6.57, P = 0.0012) in the amyloid-injected rats. (***d***) Representative path tracings in each quadrant during the probe trial on day 6 (T, target quadrant; R, right quadrant; O, opposite quadrant; L, left quadrant). Data represent mean ± s.e.m. For box-and-whiskers plots, the box extends from the 25th to 75th percentiles, a line within the box marks the median. Whiskers (error bars) above and below the box represent the minimum and maximum values. *P<0.05, **P<0.01, ***P<0.001.

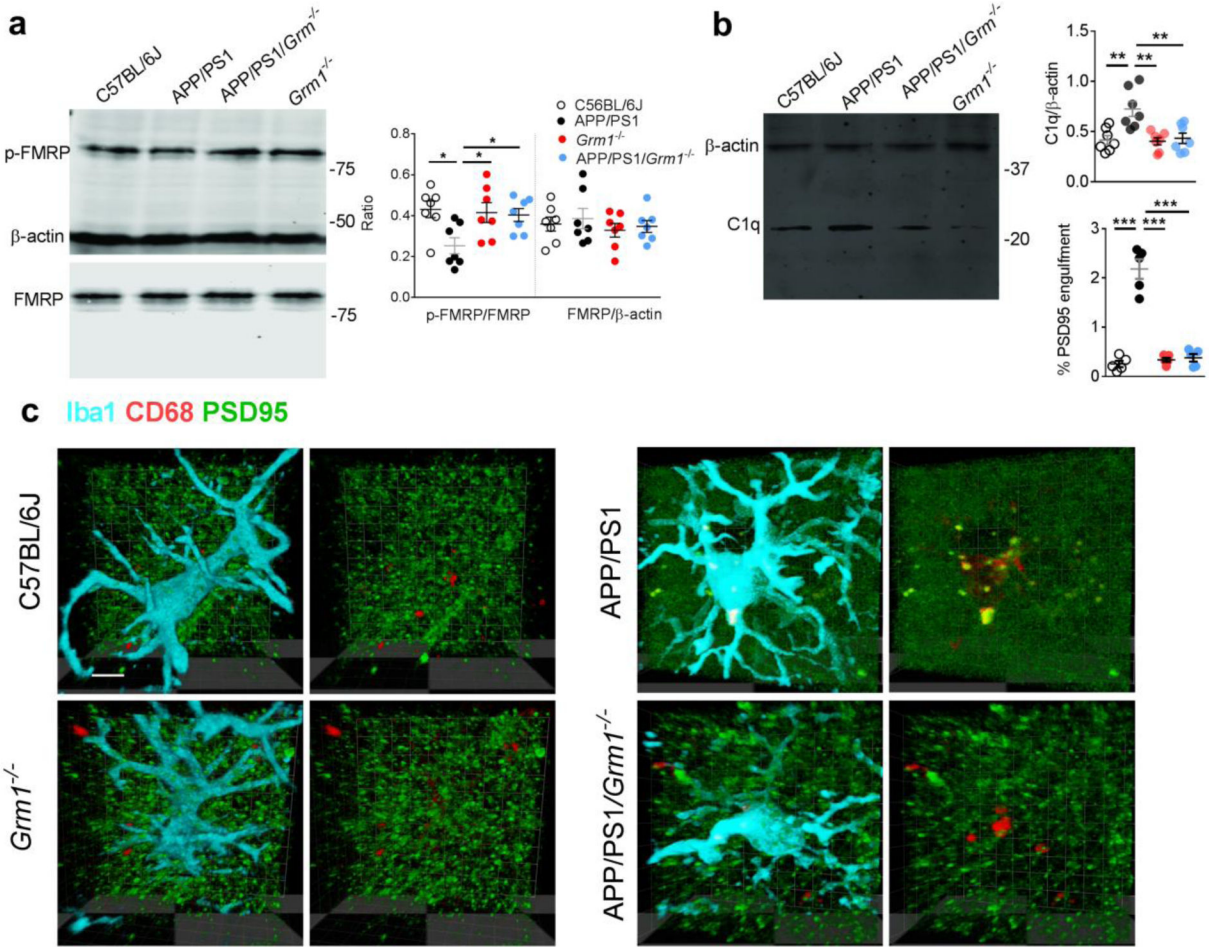

Fig 8. Knockout of mGluR1 (*Grm1*$^{-/-}$) attenuated microglial phagocytosis of synapses.

Significant dephosphorylation of p-FMRP was observed in the hippocampal CA1 synaptosome in APP/PS1 mice, which was recovered by the knockout of mGluR1 (***a***, n = 7 mice in each group, $F_{3,24} = 4.15$, P = 0.017). Knockout of mGluR1 attenuated the C1q upregulation in APP/PS1 mice (***b***, n = 7 mice in each group, $F_{3,24} = 8.39$, P = 0.0005). Knockout of mGluR1 significantly decreased the internalization of PSD95 with lysosome marker CD68 in microglia (Iba1) in APP/PS1 mice (***c***, n = 5 mice in each group, $F_{3,16} = 68.1$, P <0.0001, scale bar = 10 μm). Right micrographs were presented to show the same microglia in which only the lysosomes (red) and PSD95 (green) were visualized. Each dot represents the mean value of 4 brain sections of one animal. Data represent mean ± s.e.m. *P<0.05, **P<0.01, ***P<0.001.

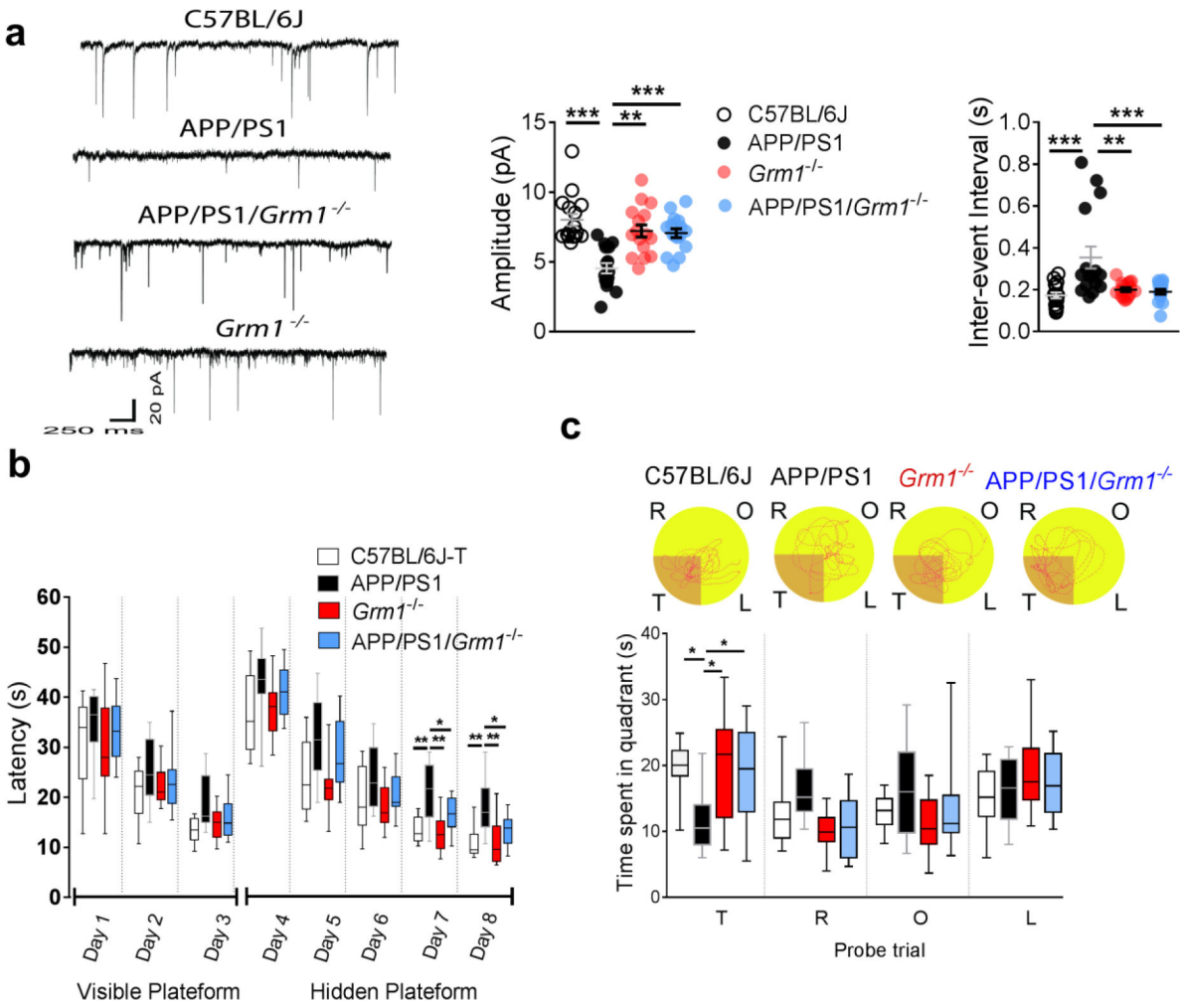

Fig 9. Knockout of mGluR1 (*Grm1*$^{-/-}$) attenuated synaptic and cognitive impairments in APP/PS1 mice.

Knockout of mGluR1 significantly recovered the amplitude (***a***, n = 16 animals in each group, Kruskal-Wallis Statistic KW = 27.1, P<0.0001) and inter-event interval of mEPSCs (***a***, n = 16 animals in each group, Kruskal-Wallis Statistic KW = 27.1, P<0.0001) in the hippocampal CA1 neurons in APP/PS1 mice. Knockout of mGluR1 shortened the escape latency in the hidden platform (***b,*** n = 10 mice in each group, effect of group [$F_{3,36}$ = 14.1, P<0.0001], effect of time [$F_{4,36}$ = 125.3, P<0.0001], interaction between group and time [P = 0.99]) and increased the time spent in the target quadrant during the probe trial (***c,*** n = 10 mice in each group, $F_{4,36}$ = 3.79, P = 0.02) in APP/PS1 mice. No difference was noted among the groups during testing in the visible platform. Representative path tracings in each quadrant during the probe trial (T, target quadrant; R, right quadrant; O, opposite quadrant; L, left quadrant). Data represent mean ± s.e.m. For box-and-whiskers plots, the box extends from the 25th to 75th percentiles, a line within the box marks the median. Whiskers (error bars) above and below the box represent the minimum and maximum values. *P<0.05, **P<0.01, ***P<0.001.

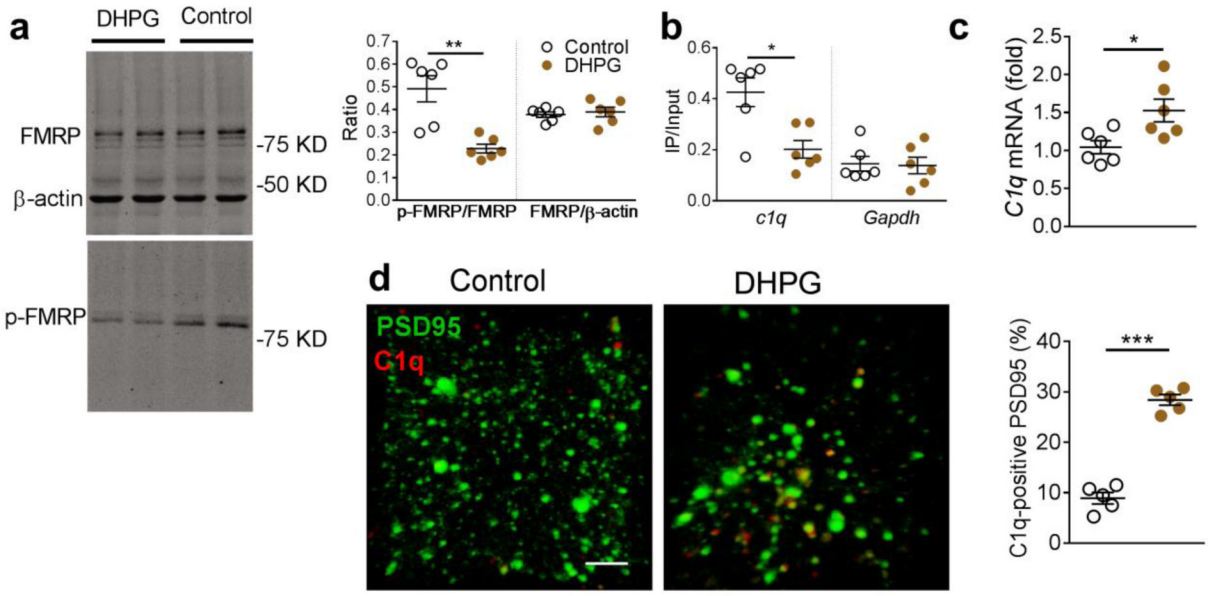

Figure 10. Activation of mGluR1 signaling by specific mGluR agonist dihydroxyphenylglycine (DHPG) upregulated hippocampal C1q expression.

Microinjection of DHPG into the hippocampal CA1 in naïve rats induced dephosphorylation of FMRP (a, n = 6 rats in each group, Mann-Whitney U-statistic = 35.00, two-tailed P = 0.007), decreased the binding between phosphorylated FMRP (p-FMRP) and *C1q* mRNA (b, n = 6 rats in each group, Mann-Whitney U-statistic = 33.00, two-tailed P = 0.015), and increased *C1q* mRNA in the hippocampal CA1 synaptosome (c, n = 6 rats in each group, t = 2.8, DF = 10, two-tailed P = 0.018). DHPG also increased the C1q immunosignal co-localized with PSD95 in the hippocampal CA1 in the naïve rats (d, n = 5 rats in each group, t = 12.6, DF = 8, two-tailed P <0.0001, scale bar = 10 μm). Each dot represents the mean value of 4 brain sections of one rat. Data represent mean ± s.e.m. *P<0.05, **P<0.01, ***P<0.001.

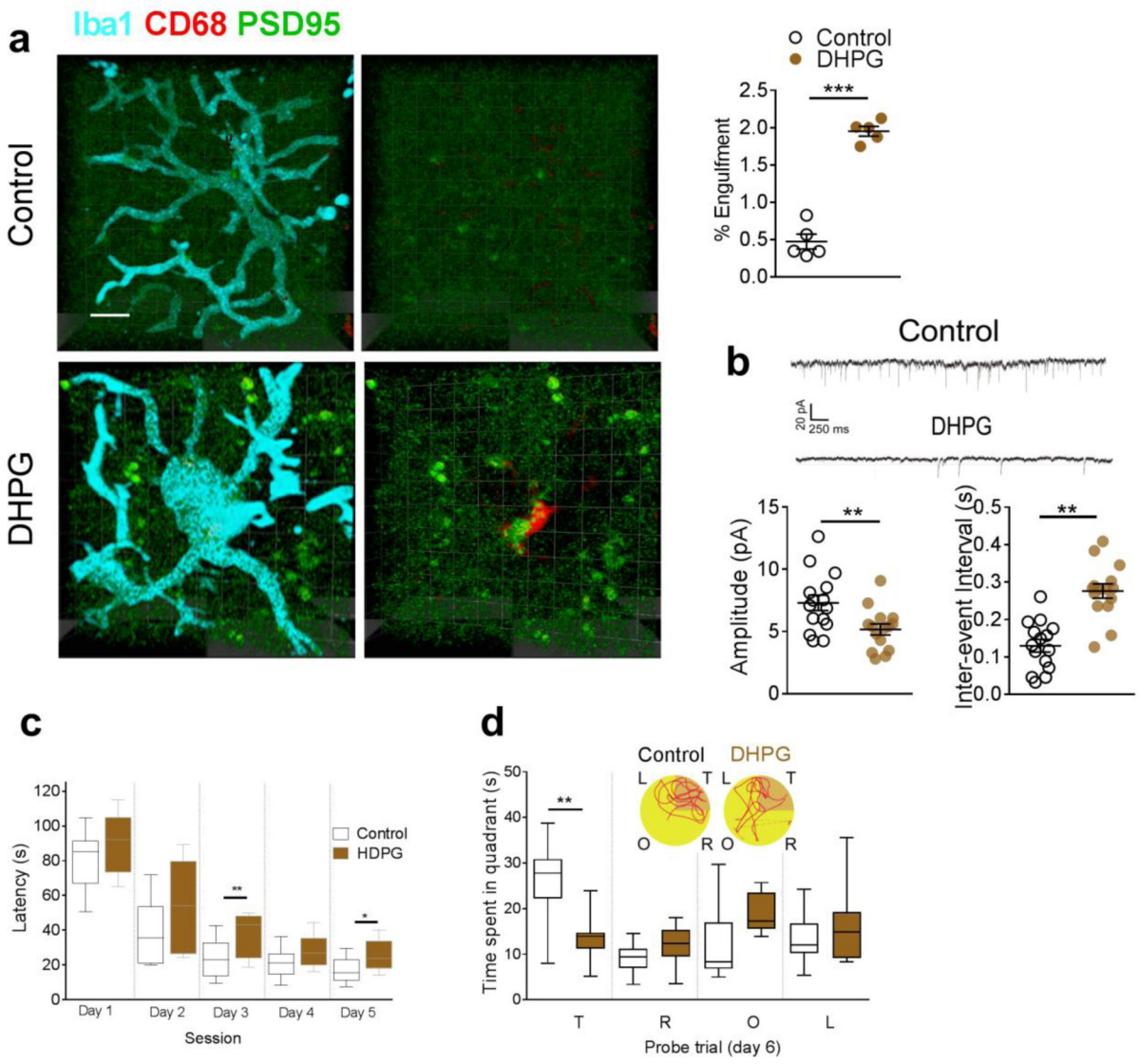

Figure 11. Activation of mGluR1 signaling by DHPG induced the microglial phagocytosis of glutamatergic synapses.

DHPG increased the internalization of PSD95 with the lysosome marker CD68 in microglia in the hippocampal CA1of naïve rats (***a***, n = 5 rats in each group, unpaired-t test, t = 12.4, DF = 8, two-tailed P <0.0001, scale bar = 10 μm). Each dot represents the mean value of 4 brain sections of one rat. DHPG also decreased the amplitude (***b***, n = 15 rats in each group, unpaired-t test, t = 2.8, DF = 28, two-tailed P = 0.0084) and increased inter-event interval (***b***, n = 15 rats in each group, unpaired-t test, t = 2.8, DF = 28, two-tailed P = 0.0084) of mEPSCs in hippocampal CA1 neurons, and increased escape latency (***c***, n = 10 rats in each group, effect of group [$F_{1,18}$ = 8.2, P = 0.01], effect of time [$F_{4,18}$ = 82.8, P<0.0001], interaction between group and time [P = 0.52]), and decreased the time in the target quadrant (***d***, n = 10 rats in each group, $F_{1,18}$ = 14.4, P = 0.001). (**d**) Representative path tracings in each quadrant during the probe trial on day 6 (T, target quadrant; R, right quadrant; O, opposite quadrant; L, left quadrant). Data represent mean ± s.e.m. For box-and-whiskers plots, the box extends from the 25th to 75th percentiles, a line within the box marks the

median. Whiskers (error bars) above and below the box represent the minimum and maximum values. *P<0.05, **P<0.01, ***P<0.001.

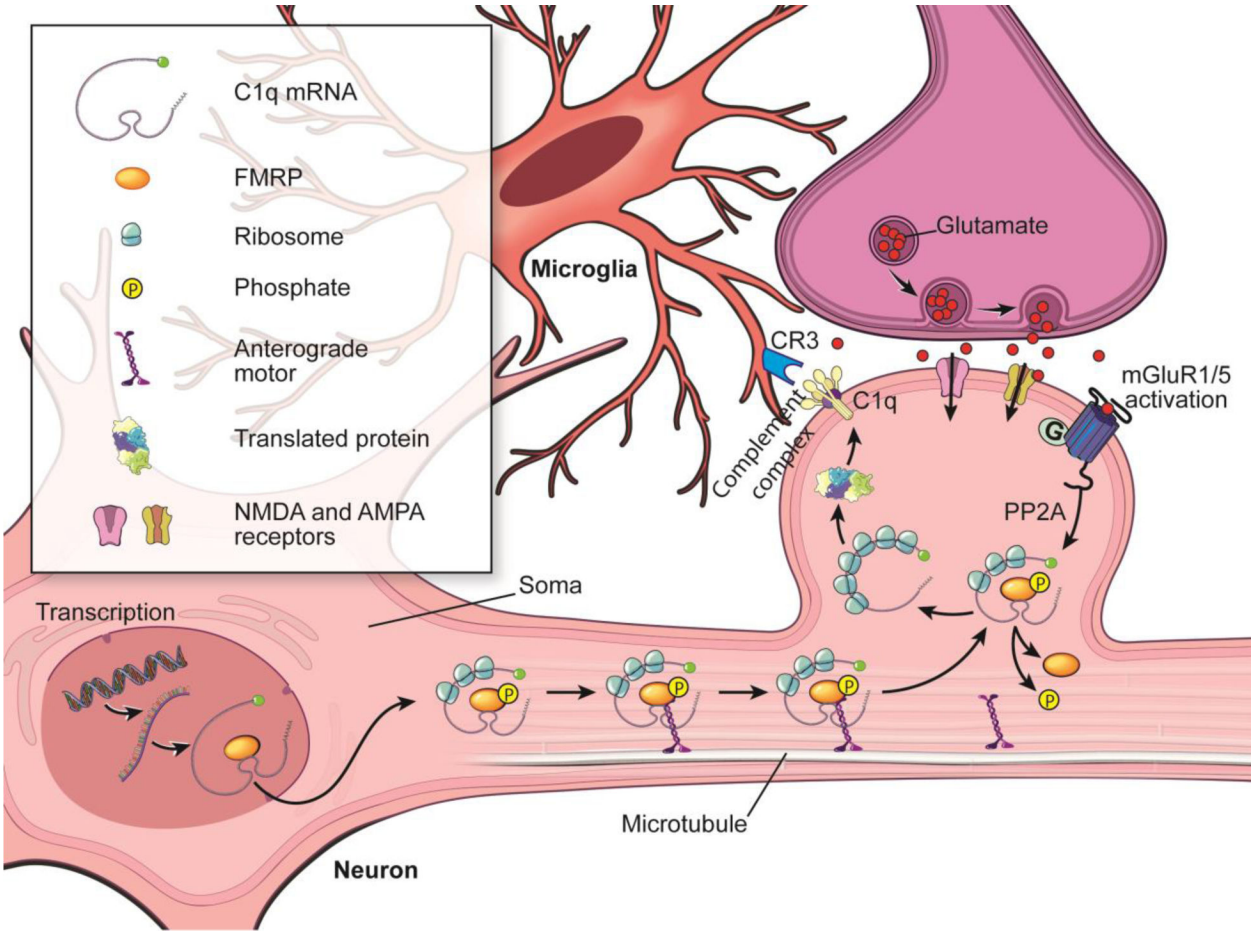

Figure 12. Diagram of the hypothesis.

Abnormal accumulation of amyloid fibrils induces substantial neuroinflammation (e.g., microglial activation) and the upregulation of mGluR1 signaling in the hippocampal CA1. Activation of mGluR1 signaling induces remarkable PP2A activity, which triggers the dephosphorylation of FMRP in the glutamatergic synapses. This adaptation of translational machinery, in turn, facilitates the transport and local translation of synaptic C1q mRNA in the glutamatergic synapses. The increased expression of C1q in glutamatergic synapses initiates the complement response leading to CR3 opsonization in the activated microglia, which eventually triggers the microglial phagocytosis of hippocampal glutamatergic synapses, thus contributing to the synaptic dysfunction and memory deficiency induced by amyloid fibrils.